PHYSICAL SCIENCES REPORT, PART 2:
DETAILED 21ST CENTURY CLIMATE PROJECTIONS FOR CAMPTON AND SURROUNDING AREA.

S. Miller
9 August 2020

Background. Future climate conditions for the region in around Campton, New Hampshire were estimated using model data provided by the Earth Systems Research Center (ESRC) at the University of New Hampshire's Institute for the Study of Earth, Oceans, and Space. This work was done to evaluate the vulnerability of Campton's local economy to stresses on the local ski industry and local agriculture, as well as the vulnerability of the town's public health brought about by anthropogenic climate change over the course of the 21st Century. The primary objective was to evaluate changes to the climate during the period beginning in 2020 and ending in 2040, which corresponds to the main focus of our report on climate change adaptation and mitigation strategies, commissioned during the 2020 Town Meeting. The secondary objective of this work was to evaluate climatic changes over the remainder of the 21st Century.

ESRC used an ensemble of 29 Global Climate Models (GCMs) to project daily values of total precipitation [mm], maximum and minimum temperature [°C], and snowpack [mm SWE[1]]. A smaller ensemble of 14 GCMs was used to project daily values of snowfall [mm SWE]. In all cases, the base GCMs were used to compute *mean* climatic conditions, to which additional processing was then applied to compute random variations about the mean conditions projected for a given day, thereby simulating weather. Data were then downscaled to local conditions via the method described in Pierce *et al.* (2014) and Grogan *et al.* (2020). Locally-downscaled conditions were computed to a resolution of 1/16 of a degree of latitude, corresponding to a linear distance of 6.9 kilometers, or about 47.8 km[2]. Time series of all five daily parameters for the gridpoints corresponding to four ski resorts within about 25 miles of Campton (Table 1) were extracted from each ensemble member by Burakowski (2020), and made available via electronic bulletin board. Miller downloaded the files and used a Matlab-based suite of data analysis procedures, called *AirSea*, to compute ensemble means and associated statistics (Miller 2020). Additional parameters were computed using *AirSea* from the five original parameters as described below (see Data and Methods).

Table 1: Ski resorts corresponding to gridpoints used in this study.

Name of Resort	Latitude [DMS N]	Longitude [DMS W]	Distance from Campton [km][2] (miles)
Cannon Mountain	44° 10' 37"	71° 42' 06"	36.61 (22.75)
Loon Mountain	44° 03' 23"	71° 38' 00"	22.99 (14.29)
Tenney Mountain	43° 44' 49"	71° 45' 55"	14.78 (9.18)
Waterville Valley	43° 57' 06"	71° 30' 18"	16.12 (10.02)

All models in the ensemble were forced using two different greenhouse concentration scenarios, known as "Representative Concentration Pathways" (RCPs; Grogan *et al.* 2020). These are not emissions scenarios, but models of greenhouse gas concentration levels that result in different levels of radiative

[1] SWE = Snow Water Equivalent; the amount of liquid water obtained if the frozen sample is melted.
[2] Campton coordinates (43° 50' 59" N, 71° 38' 54" W) correspond to Town Hall, near Exit 28 on I-93.

forcing, and were adopted for use with GCMs by scientists contributing to the work of the Intergovernmental Panel on Climate Change (IPCC). While there are many RCPs, only four were used in the IPCC's Fifth Assessment, published in 2014: RCP2.6, RCP4.5, RCP6.0, and RCP 8.5. Figure 1 (below) shows all four RCPs and their corresponding greenhouse concentration levels for the period beginning in 2000 CE and ending in 2100 CE. For more detail, the reader is referred to the IPCC's Data Distribution Center (2019), and the RCP Database (2009). For the relationship between RCPs and socioeconomic conditions, please see Hausfather (2018).

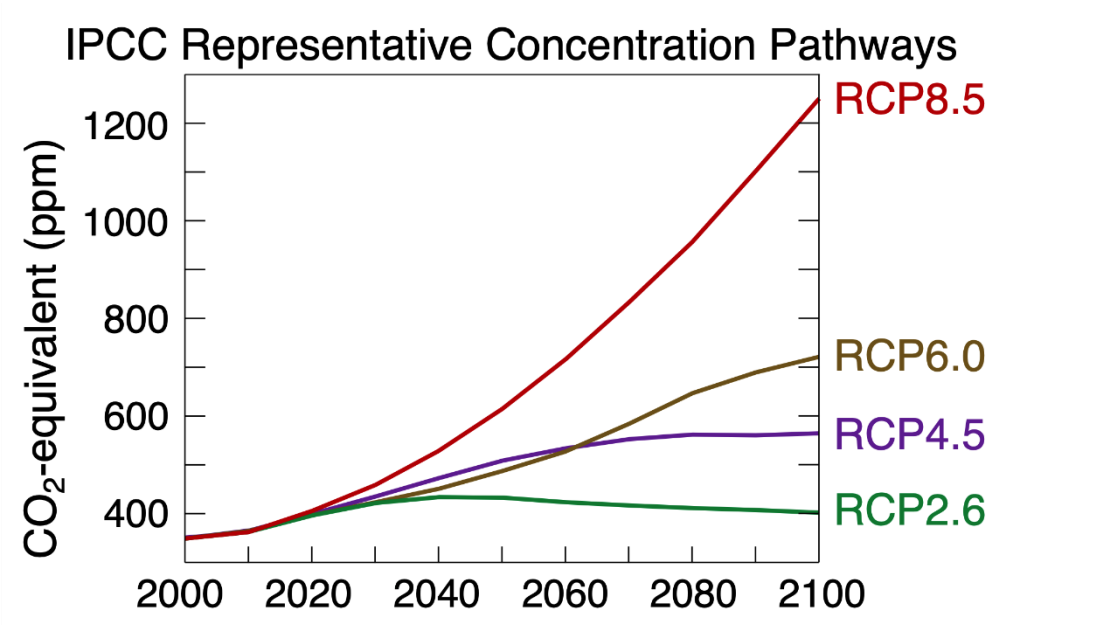

Fig. 1: IPCC Representative Concentration Pathways (Creative Commons License 4.0). Horizontal axis indicates year; vertical axis indicates corresponding CO_2-equivalent GHG concentration [ppmv].

The two RCPS used with the model ensemble in this work are further defined by the National Oceanic and Atmospheric Administration (NOAA(a) n.d.; NOAA(b) n.d.) as follows:

- RCP4.5 is "a stabilization scenario, which means the radiative forcing level stabilizes at 4.5 Wm^{-2} before 2100 by [the] employment of a range of technologies and strategies for reducing greenhouse gas emissions." This can be thought of as a scenario in which very aggressive actions are taken at all levels of society, worldwide, to reduce anthropogenic greenhouse gas emissions and stabilize the climate in Holocene-like conditions. This might also be described as the "Earth System Stewardship" scenario, described in Steffen *et al.* (2018).

- RCP8.5 is a "scenario [in which] the radiative forcing reaches 8.5 Wm^{-2} characterized by increased greenhouse gas emissions over time [and is] representative for scenarios in the literature leading to high greenhouse [gas] concentration levels." This has been described as a "business as usual" scenario, in which anthropogenic greenhouse gas emissions continue to grow as a result of increasing industrialization, large-scale agriculture, population growth, and rising standards of living in the developing world. There is some debate about this characterization, with some

preferring to describe RCP8.5 as "worst case scenario." It seems possible that both of these descriptions are accurate. The reader is referred to ClimateNexus (n.d.) for further discussion of this point. In Steffen *et al.* (2018), a "business as usual" RCP corresponds to the pathway leading the global climate beyond a planetary threshold, where intrinsic feedbacks carry the system into a highly stable (long-duration) "Hothouse Earth" state.

The answers to two general categories of questions were explored using the datafiles provided by UNH. These included questions about (1) how the cold-season would evolve in the Campton area over the 21st Century, and how these changes might affect recreational skiing, which is a major factor in the economy of the town; and (2) how the warm-season would evolve during the same period of time, and how these changes might impact public health, agriculture, and infrastructure. The ski season in New Hampshire usually begins in mid-November, and ends in mid-April (public domain sources), and so we defined the cold-season as the six-month period including November, December, January, February, March, and April. The warm-season was then defined as the other six-month period, beginning in May and ending in October.

Data and Methods. Burakowski (2020) provided time series of daily maximum and minimum temperature [°C], precipitation [mm], snowfall [mm SWE], and snowpack [mm SWE]. These files contained a date-time group [YYYYMMDD] in column 1, and an additional column with the parameter in question. Metadata at the top of each file listed the datatypes and applicable units. The data begin on 01 January 1980, and end on 31 December 2099. Entries are on a daily basis. The entries for the first 25 years represent observations during the "spin up" time for the ensemble's member models, and the remainder of the data are the generated by the GCMs (with additional processing for weather variations) in question (Burakowski 2020).

Individual results were computed at five-year intervals[3] from the base model data as follows:

1. Mean daily minimum temperatures by month for the cold-season were computed by (1) stepping through each ensemble member and identifying all entries for that month; (2) taking the model's mean value for the minimum temperature during that month; (3) repeating for all ensemble members; and (4) taking the ensemble-mean of all mean monthly minimum temperatures.

2. Daily maximum temperature datafiles were used to compute the number of warm-season days with high temperatures ≥ 90 °F (32.2 °C), defined at this level because it is associated with a marked increase in heat-related illness. This was accomplished by (1) stepping through each model identifying all warm-season daily high temperatures during the year in question; (2) counting the number of days during the warm-season when the high temperature met or exceeded the threshold; (3) repeating for all ensemble members; and (4) taking the ensemble-mean of all members during the warm-season for that year.

3. The mean number of days per month when artificial snowmaking is possible during the cold-season were computed using the assumption that "snow guns" can be used when the minimum temperature of the day is ≤ 28 °F (-2 °C) (Wilson *et al.* 2018; Grogan *et al.* 2020). Note that this

[3] Data in the base files were provided for *each* year. The decision to compute results at 5-yr intervals was made to reduce processor time.

criteria does not determine *how many hours* during a given day snowmaking will be possible, but only that snowmaking will be possible for at least one hour during a given day. Days during a given month with minimum temperature ≤ -2 °C were totaled up for each model, then averaged across all ensemble members for that month.

4. Mean monthly precipitation totals during the cold-season were computed by (1) stepping through each ensemble member and totaling up all precipitation values for that month; (2) repeating for all ensemble members; and (3) taking the ensemble-mean of all monthly precipitation totals.

5. Mean monthly snowfall totals were computed by similar means.

6. Mean monthly snowfall-to-precipitation ratio was computed by combining the results of steps 4 and 5 (described above), and applying the results to:

$$Ratio = 100\ \% \ x \left(\frac{Monthly\ Snowfall\ Total}{Monthly\ Precipitation\ Total}\right) \quad (1)$$

7. Mean monthly snowpack during the cold-season was computed by (1) stepping through each ensemble member and identifying all entries for that month; (2) taking the model's mean value for the daily snowpack during that month; (3) repeating for all ensemble members; and (4) taking the ensemble-mean of all mean monthly snowpack values.

8. Mean "drought lengths" were computed for the warm-season by (1) identifying stretches of days in each ensemble member with zero precipitation for 3, 5, 7…. 15 days; (2) counting them up; and (3) averaging the results for each category across all ensemble members. For example, a stretch of days with no precipitation for five days would contain three 3-day stretches, two 4-day stretches, and one 5-day stretch.

9. Warm-season heavy precipitation days were computed in "buckets," by (1) searching each ensemble-member for days with precipitation totals in certain categories (defined below); and (2) averaging the category totals across all members of the ensemble.

Cold-Season Results. In all cases, two separate sets of results are shown, corresponding to the RCP4.5 and RCP8.5 emissions scenarios. These are presented here graphically. Interpretation of these results is in the next section.

1. Average minimum daily temperature:

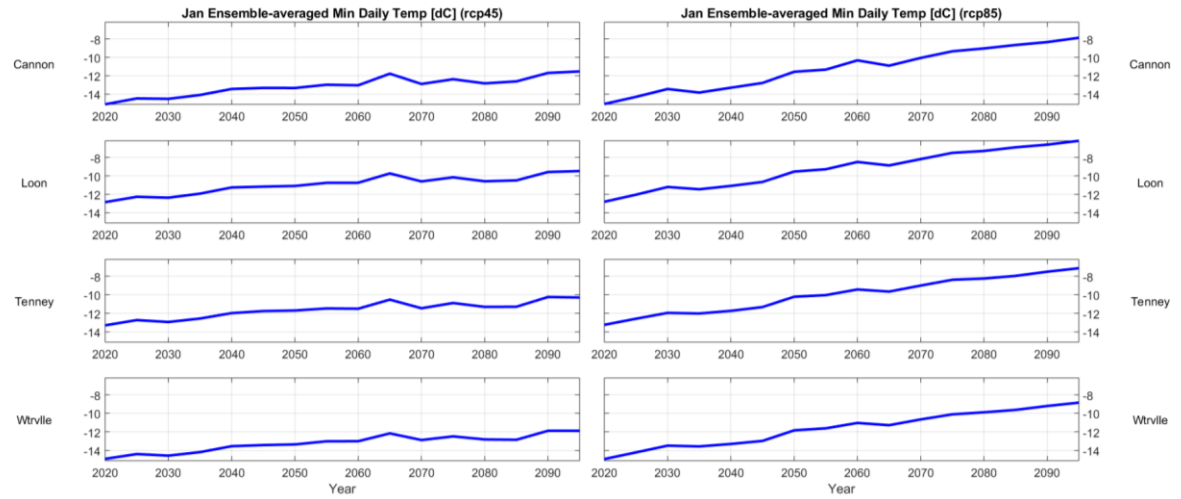

Fig. 2.1.1.: January ensemble-averaged minimum daily temperature, 2020 – 2095. Left column corresponds to RCP4.5; right column to RCP8.5. Rows correspond to different locations. Horizontal axis is years; vertical axis is temperature [°C].

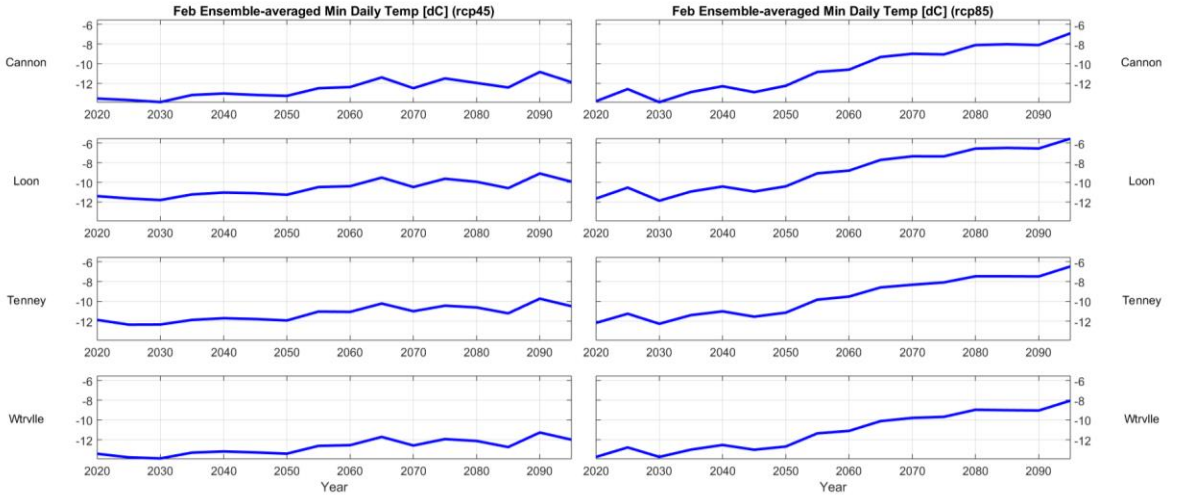

Fig. 2.1.2.: February ensemble-averaged minimum daily temperature, 2020 – 2095.

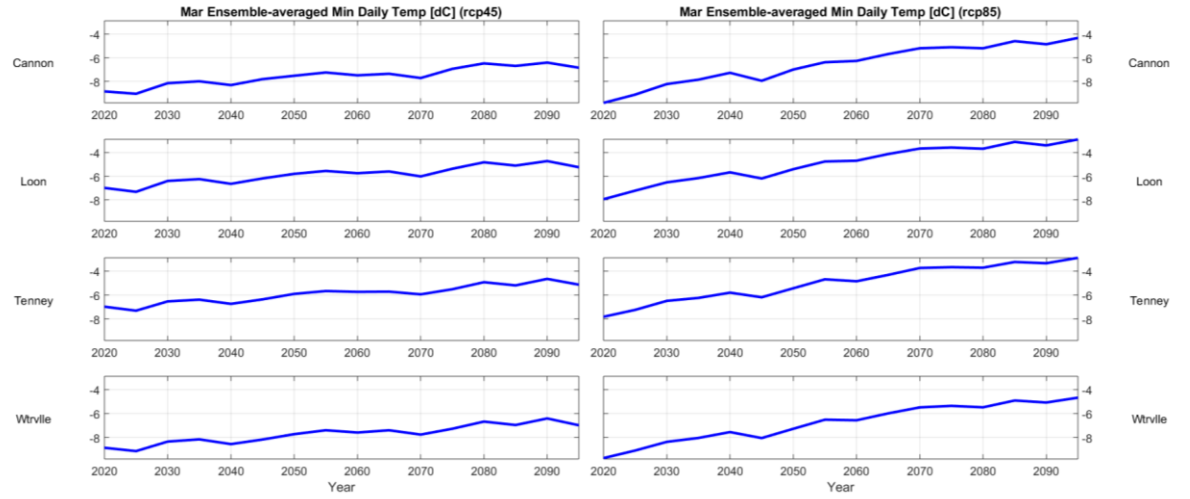

Fig. 2.1.3.: March ensemble-averaged minimum daily temperature, 2020 – 2095.

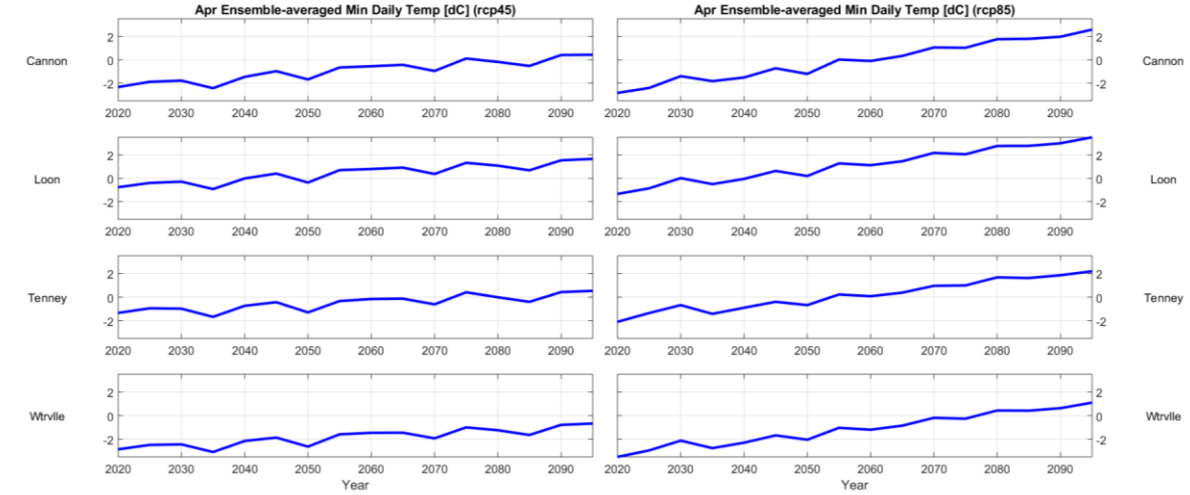

Fig. 2.1.4.: April ensemble-averaged minimum daily temperature, 2020 – 2095.

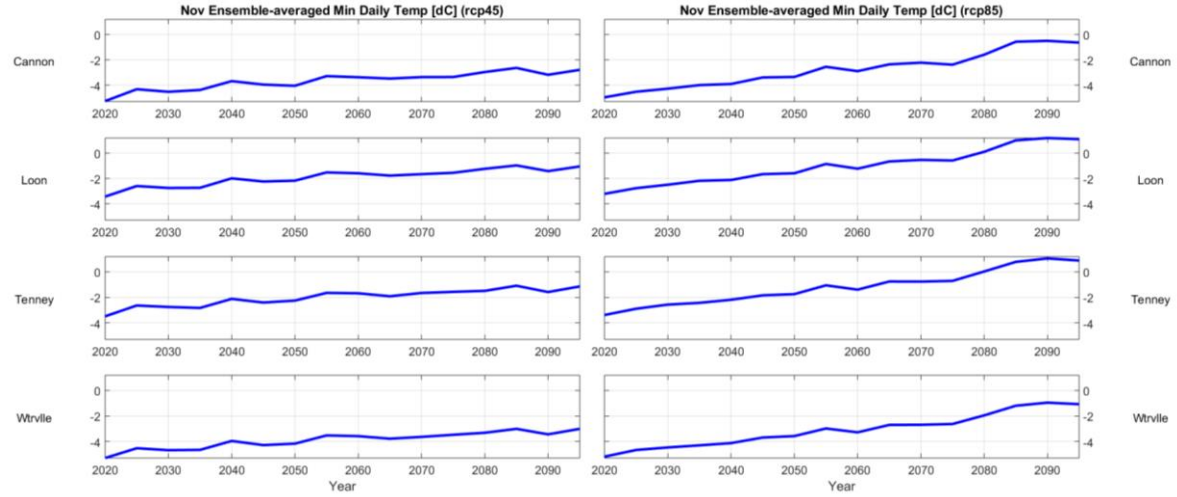

Fig. 2.1.5.: November ensemble-averaged minimum daily temperature, 2020 – 2095.

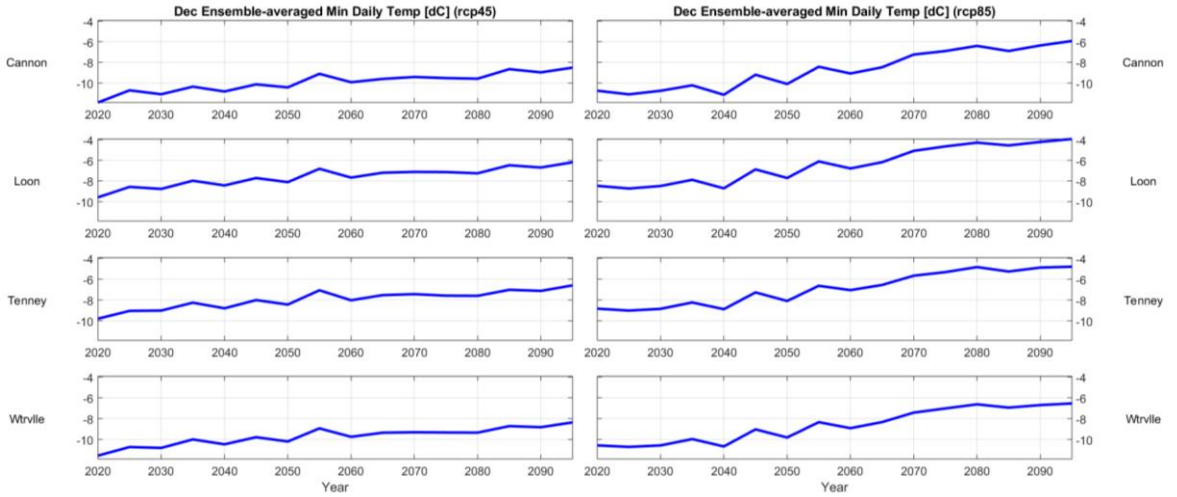

Fig. 2.1.6.: December ensemble-averaged minimum daily temperature, 2020 – 2095.

2. Average number of days when snowmaking is possible (minimum temperature ≤ 28 °F, or ≤ -2 °C):

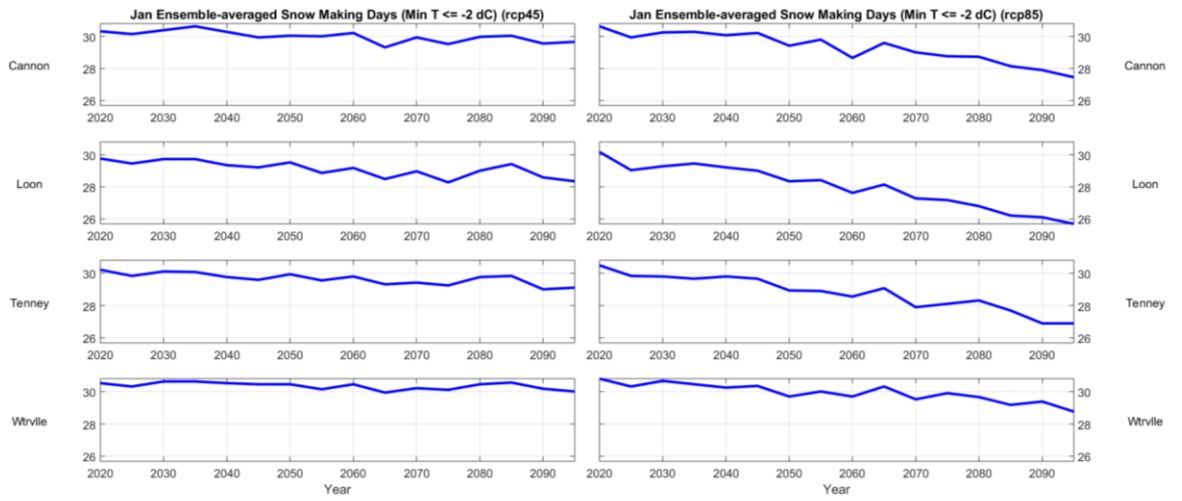

Fig. 2.2.1.: January ensemble-averaged number of days when snowmaking is possible, 2020 – 2095. Left column corresponds to RCP4.5; right column to RCP8.5. Rows correspond to different locations. Horizontal axis is years; vertical axis is number of days during the month when snowmaking is viable.

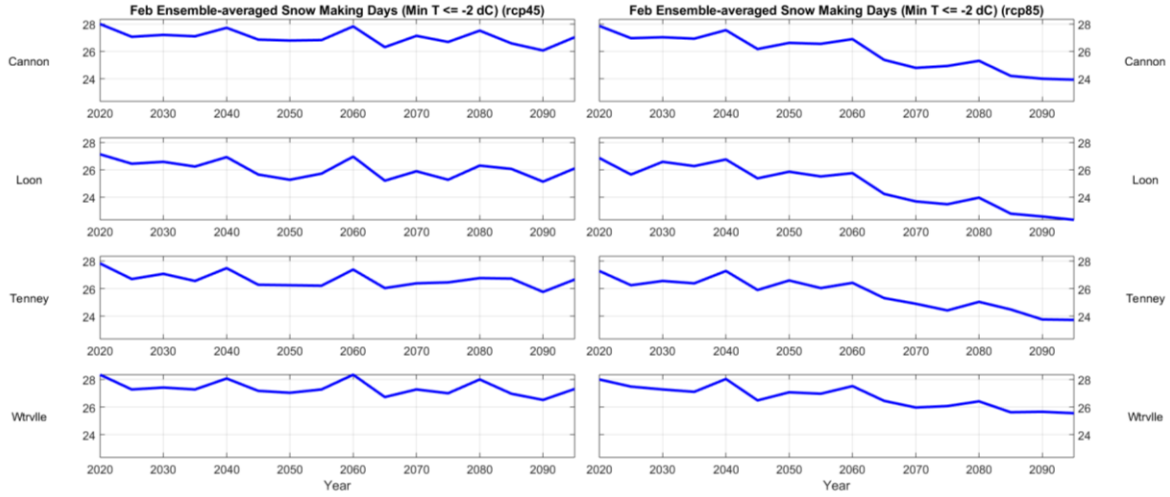

Fig. 2.2.2.: February ensemble-averaged number of days when snowmaking is possible, 2020 – 2095.

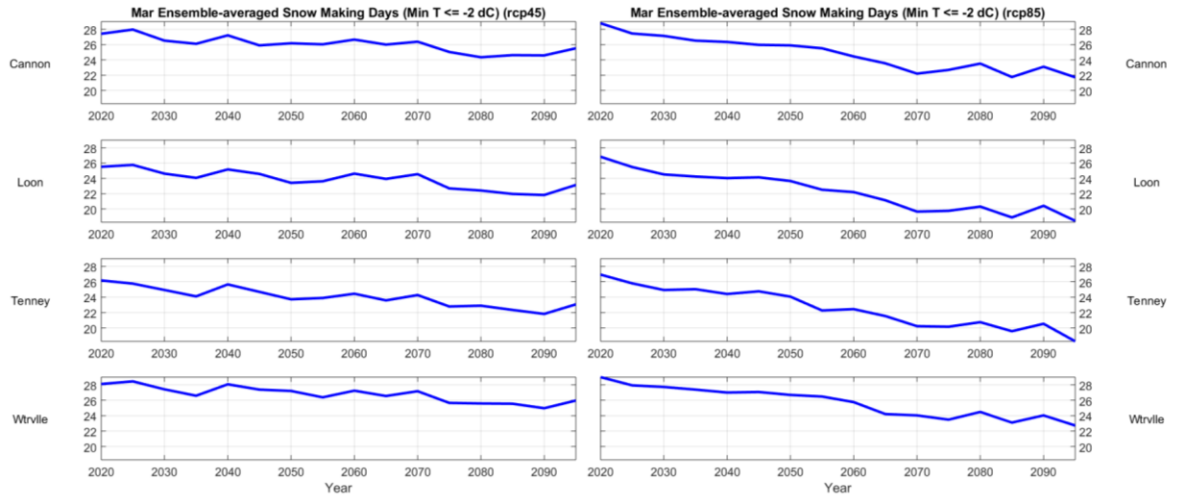

Fig. 2.2.3.: March ensemble-averaged number of days when snowmaking is possible, 2020 – 2095.

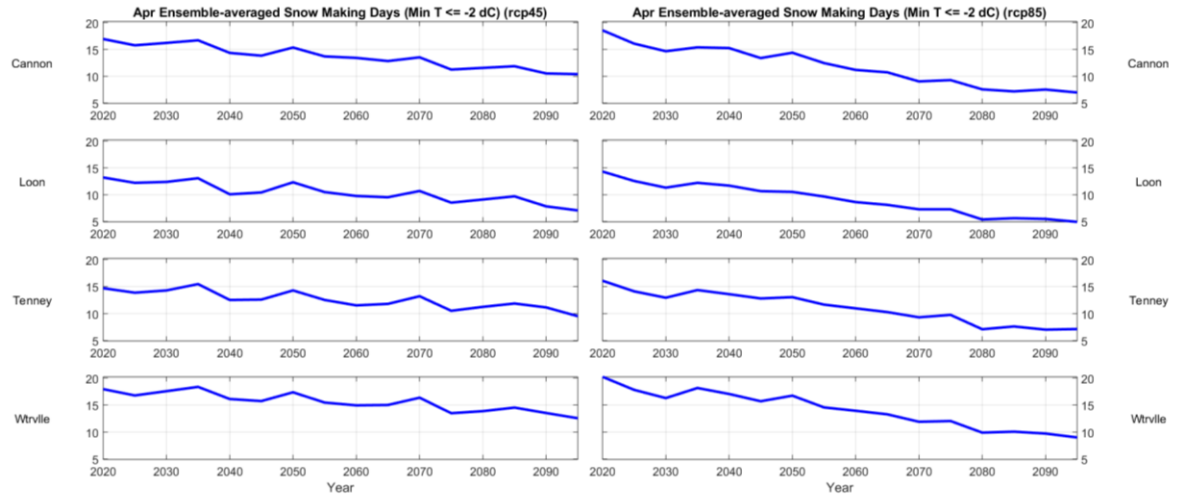

Fig. 2.2.4.: April ensemble-averaged number of days when snowmaking is possible, 2020 – 2095.

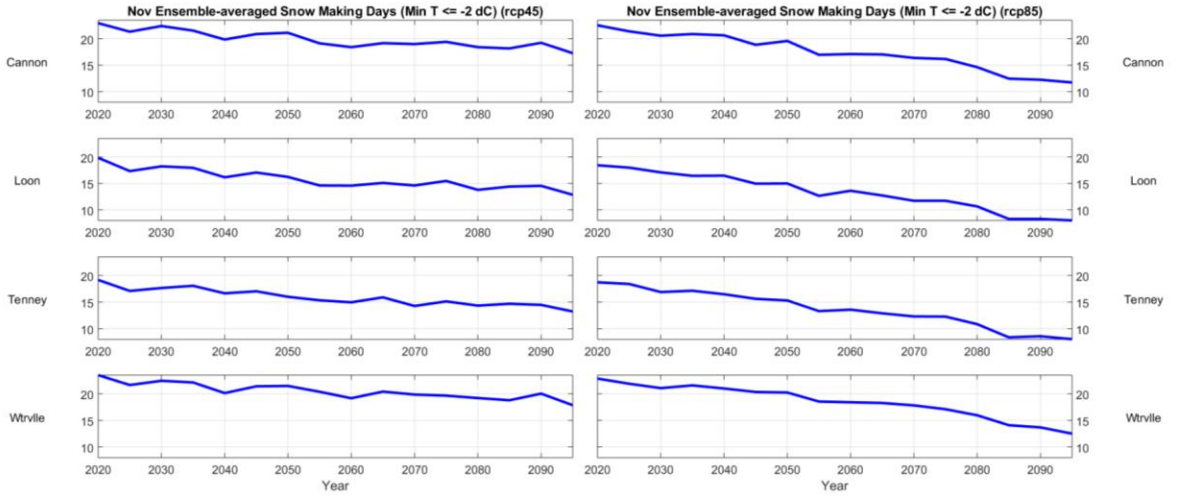

Fig. 2.2.5.: November ensemble-averaged number of days when snowmaking is possible, 2020 – 2095.

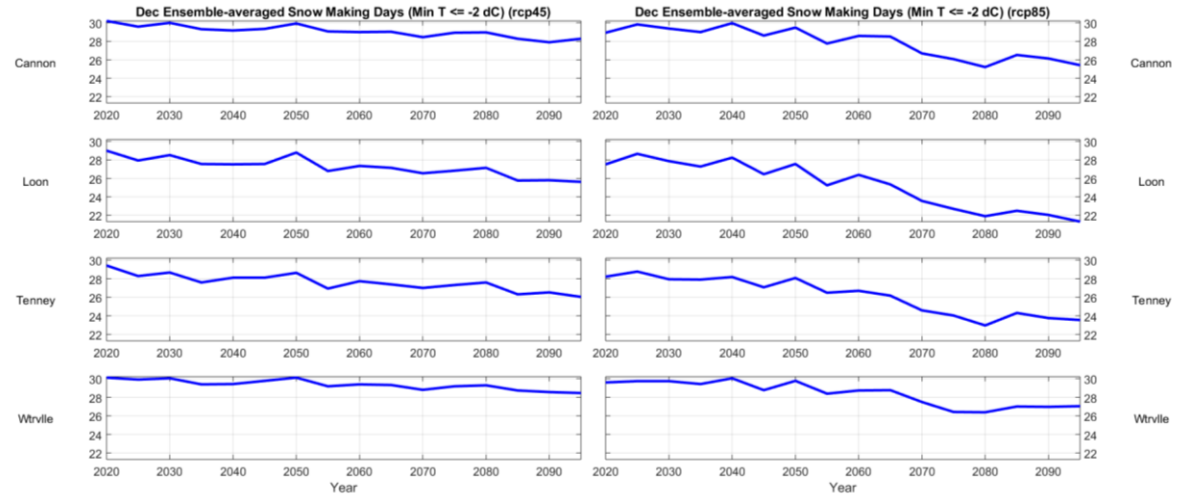

Fig. 2.2.6.: December ensemble-averaged number of days when snowmaking is possible, 2020 – 2095.

3. Total monthly snowfall:

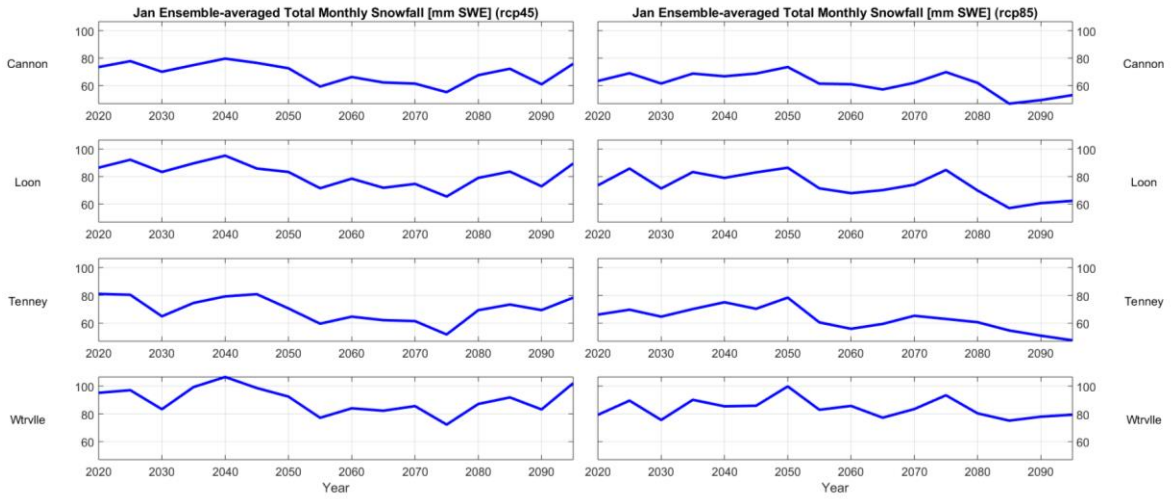

Fig. 2.3.1.: January ensemble-averaged total monthly snowfall, 2020 – 2095. Left column corresponds to RCP4.5; right column to RCP8.5. Rows correspond to different locations. Horizontal axis is years; vertical axis is total monthly snowfall [mm SWE].

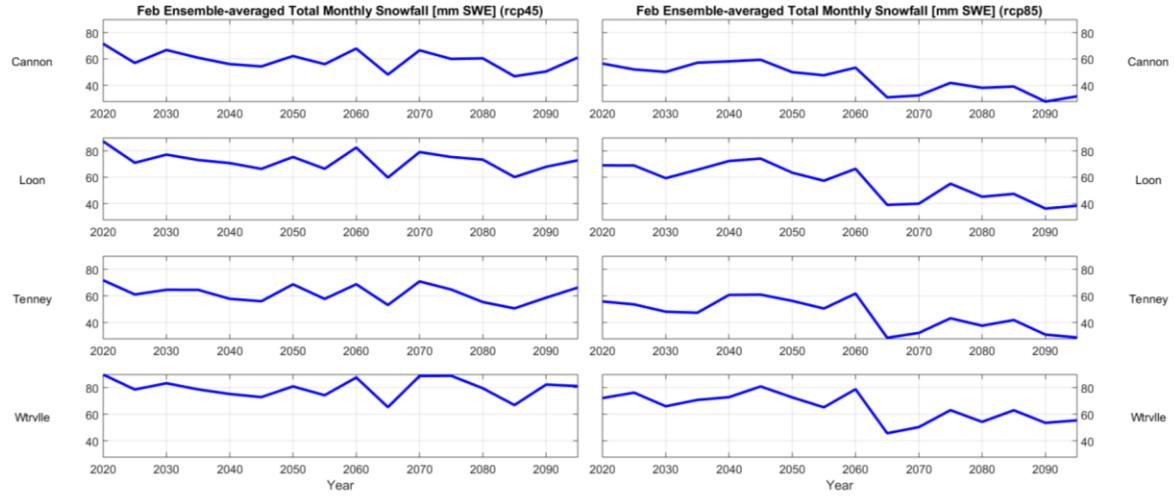

Fig. 2.3.2.: February ensemble-averaged total monthly snowfall, 2020 – 2095.

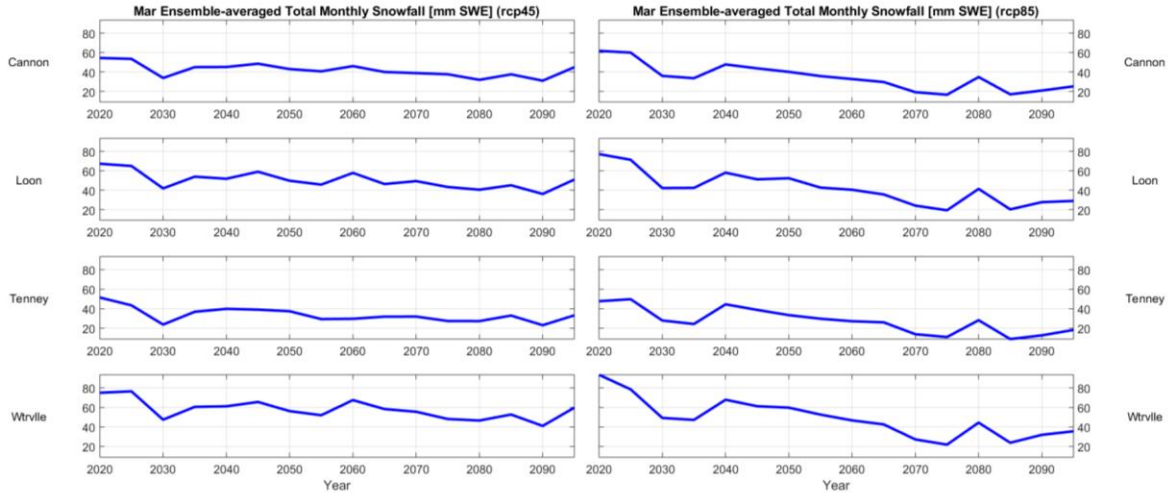

Fig. 2.3.3.: March ensemble-averaged total monthly snowfall, 2020 – 2095.

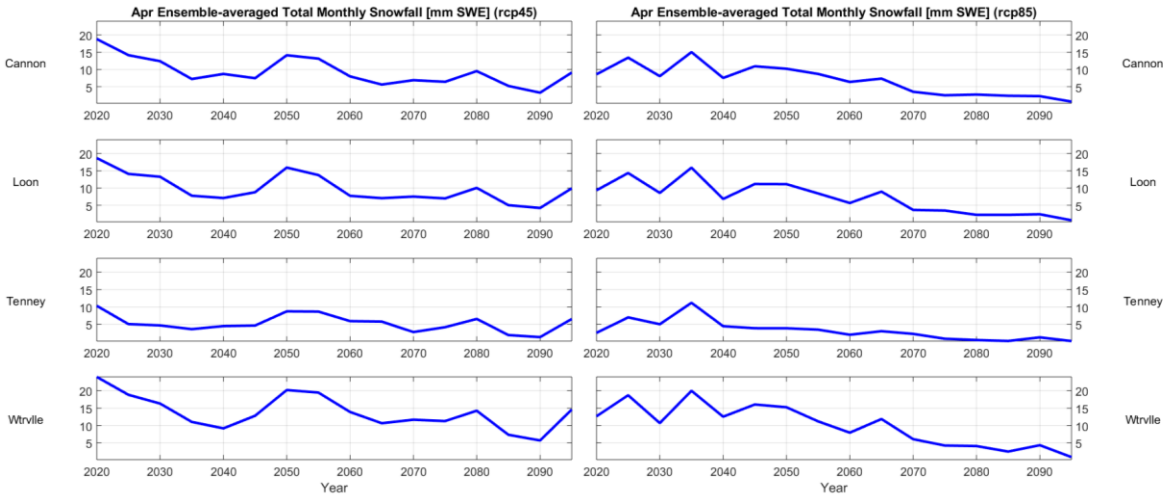

Fig. 2.3.4.: April ensemble-averaged total monthly snowfall, 2020 – 2095.

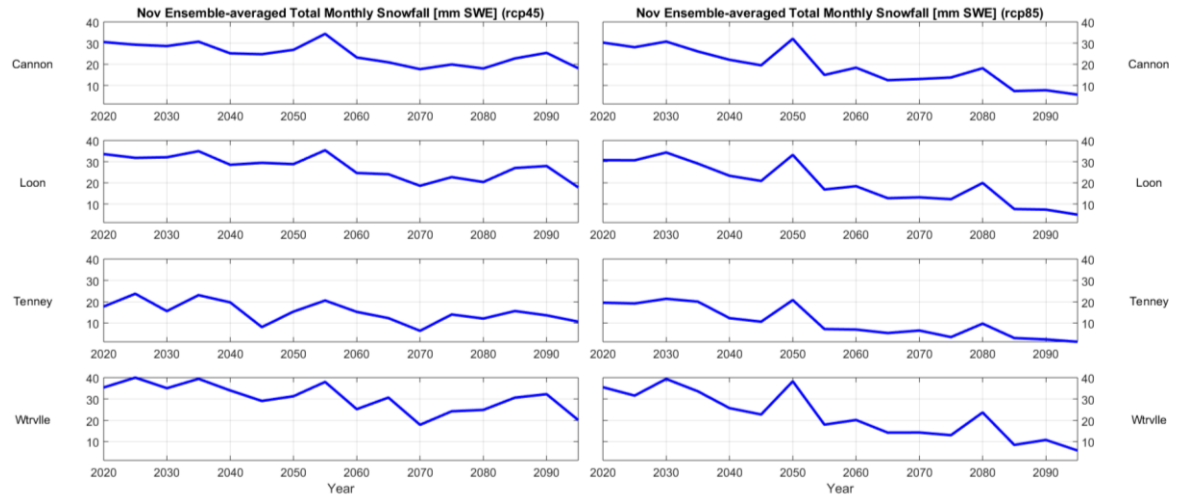

Fig. 2.3.5.: November ensemble-averaged total monthly snowfall, 2020 – 2095.

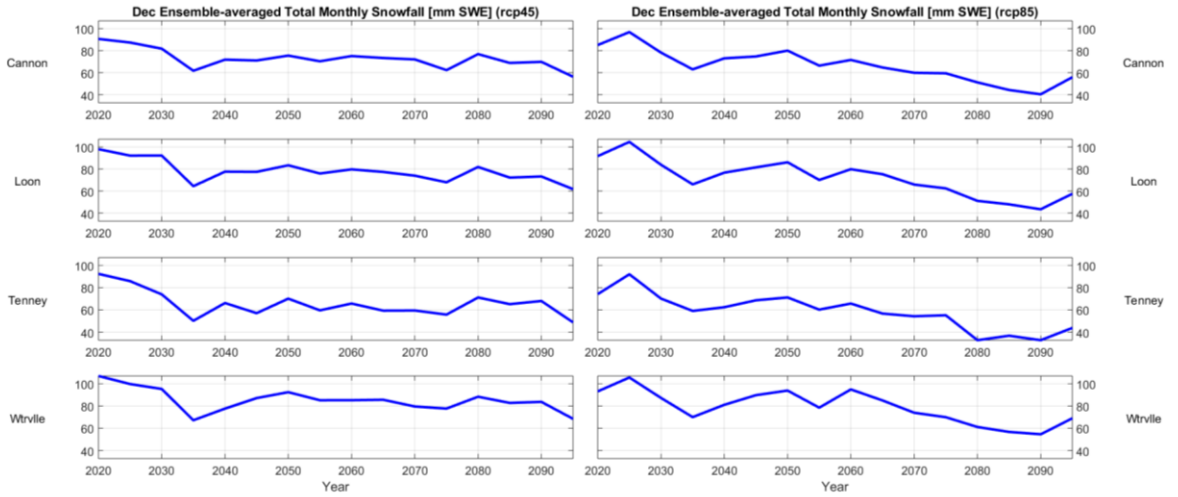

Fig. 2.3.6.: December ensemble-averaged total monthly snowfall, 2020 – 2095.

4. Average snowfall-to-total precipitation ratio:

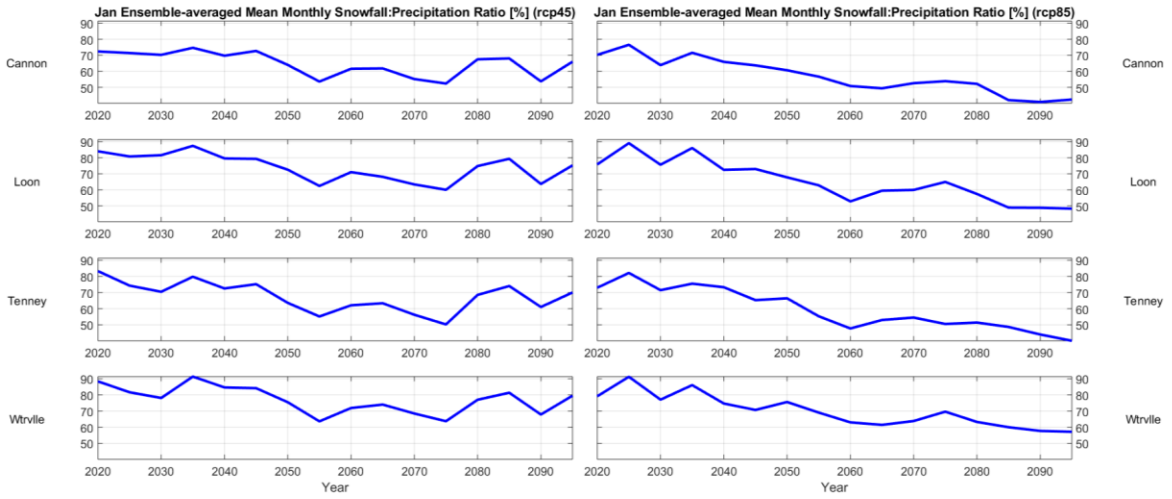

Fig. 2.4.1.: January ensemble-averaged snowfall-to-total precipitation ratio, 2020 – 2095. Left column corresponds to RCP4.5; right column to RCP8.5. Rows correspond to different locations. Horizontal axis is years; vertical axis is portion of total monthly precipitation falling as snow [%].

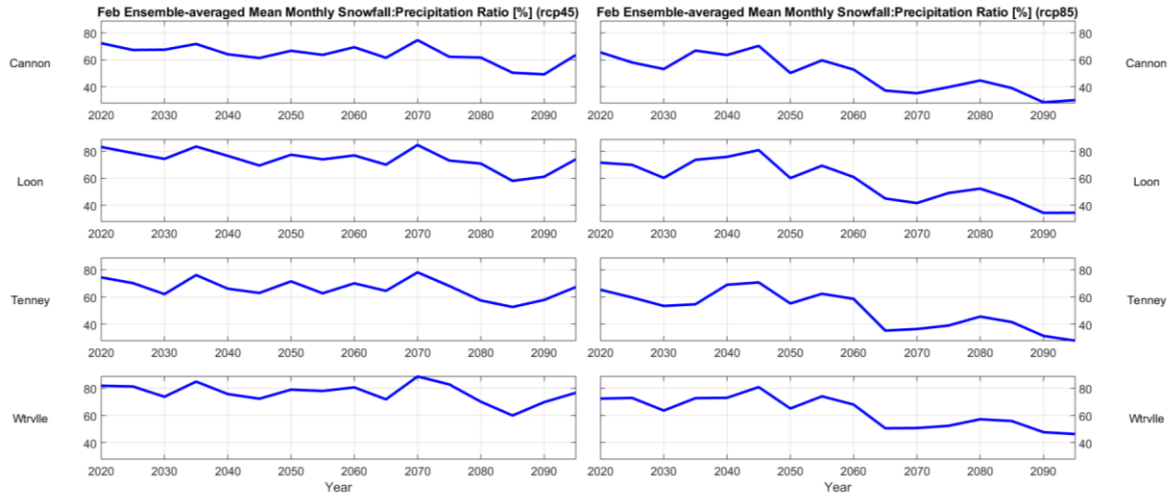

Fig. 2.4.2.: February ensemble-averaged snowfall-to-total precipitation ratio, 2020 – 2095.

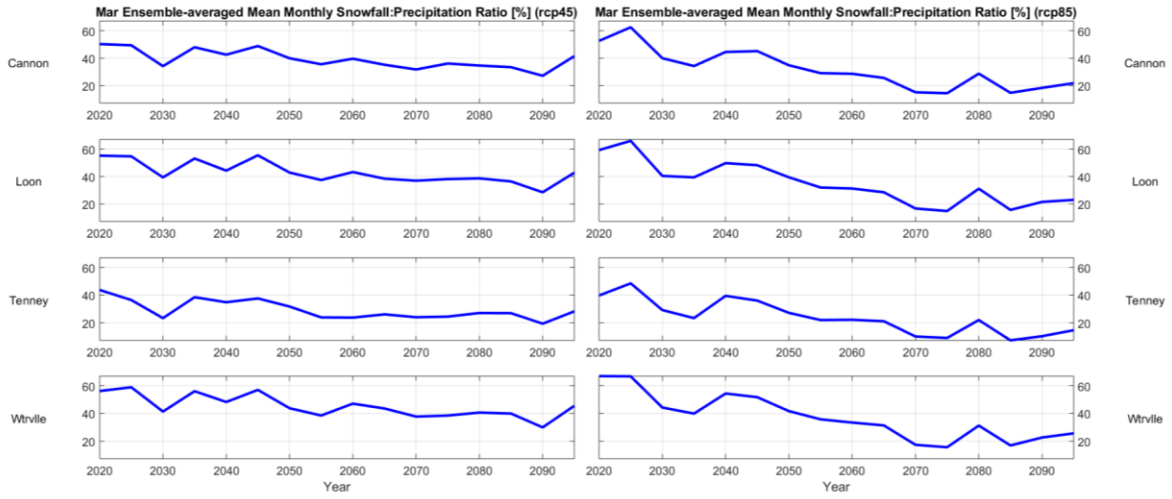

Fig. 2.4.3.: March ensemble-averaged snowfall-to-total precipitation ratio, 2020 – 2095.

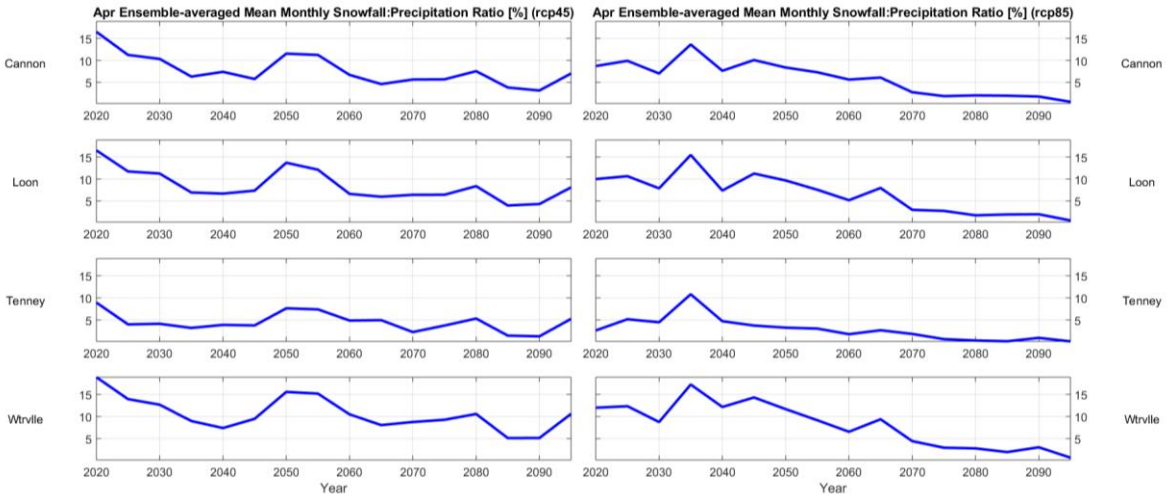

Fig. 2.4.4.: April ensemble-averaged snowfall-to-total precipitation ratio, 2020 – 2095.

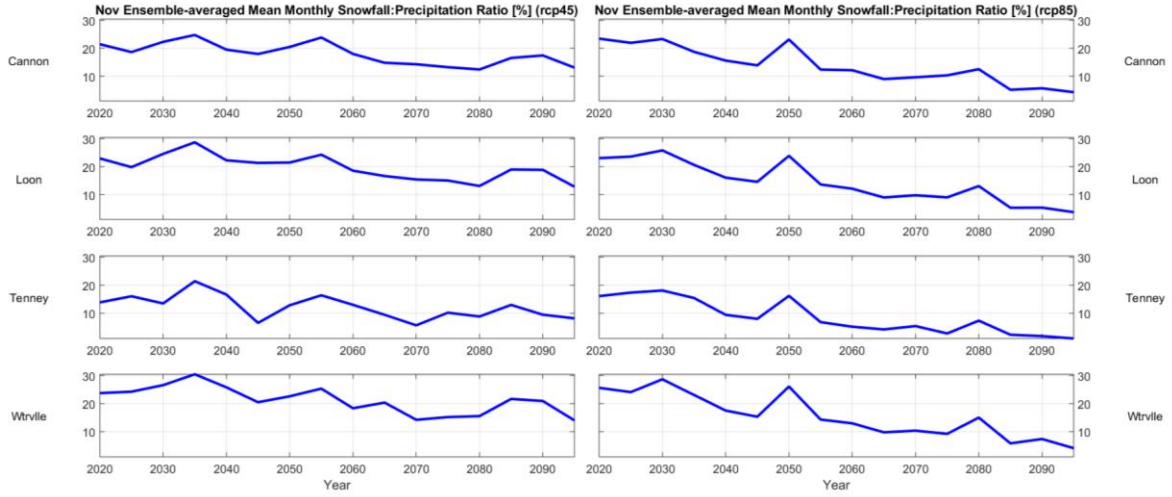

Fig. 2.4.5.: November ensemble-averaged snowfall-to-total precipitation ratio, 2020 – 2095.

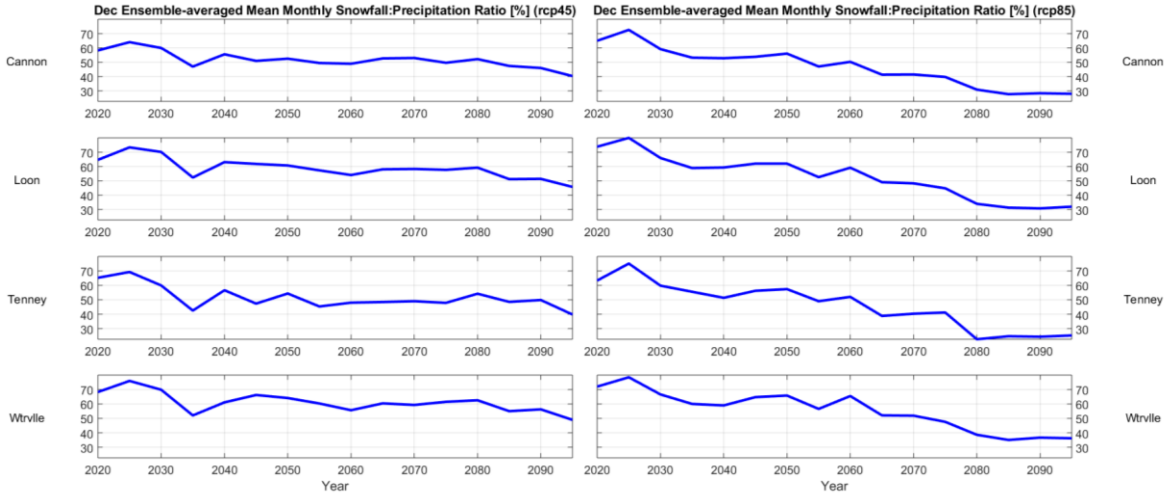

Fig. 2.4.6.: December ensemble-averaged snowfall-to-total precipitation ratio, 2020 – 2095.

5. Average natural snowpack:

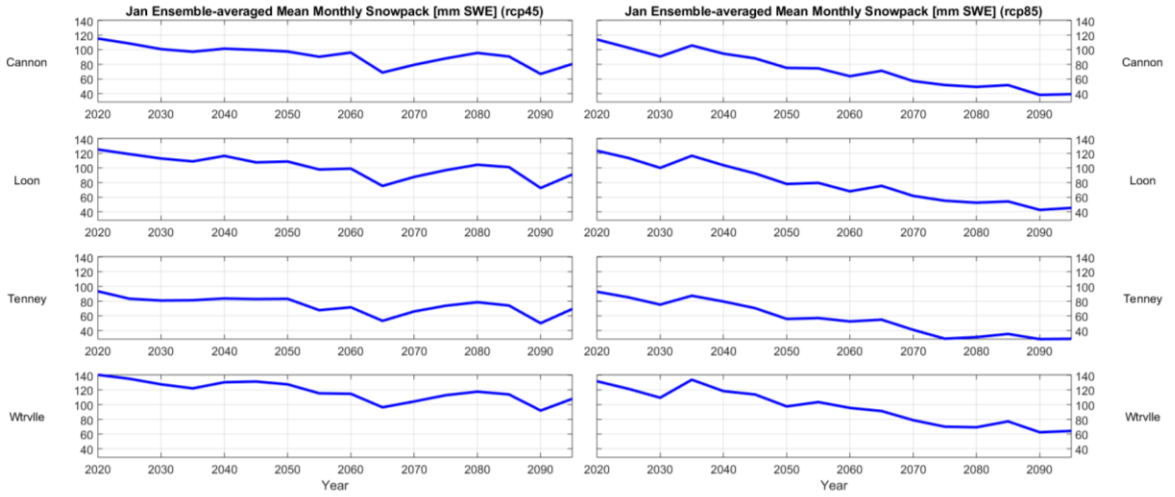

Fig. 2.5.1.: January ensemble-averaged mean monthly natural snowpack, 2020 – 2095. Left column corresponds to RCP4.5; right column to RCP8.5. Rows correspond to different locations. Horizontal axis is years; vertical axis is natural snowpack [mm SWE].

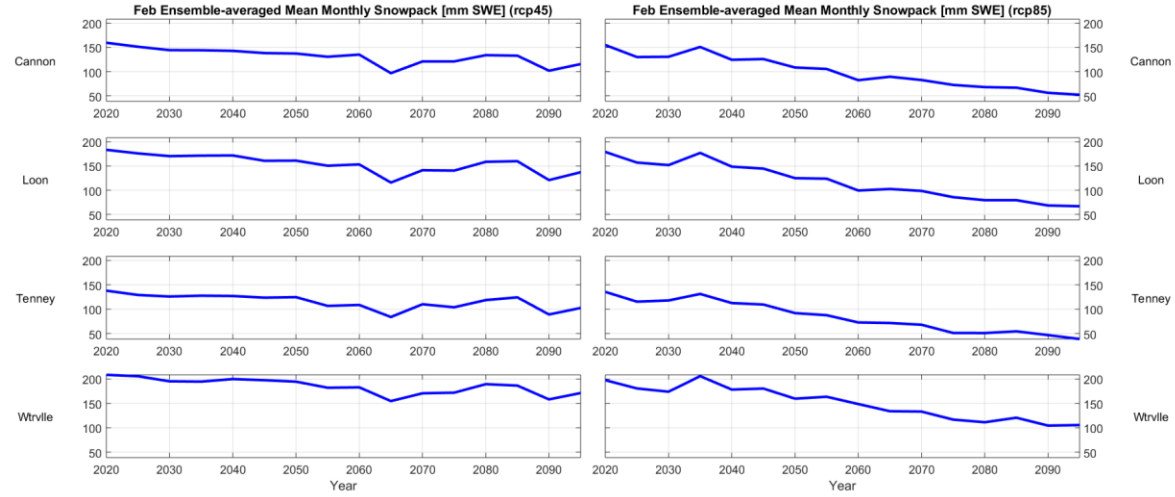

Fig. 2.5.2.: February ensemble-averaged mean monthly natural snowpack, 2020 – 2095.

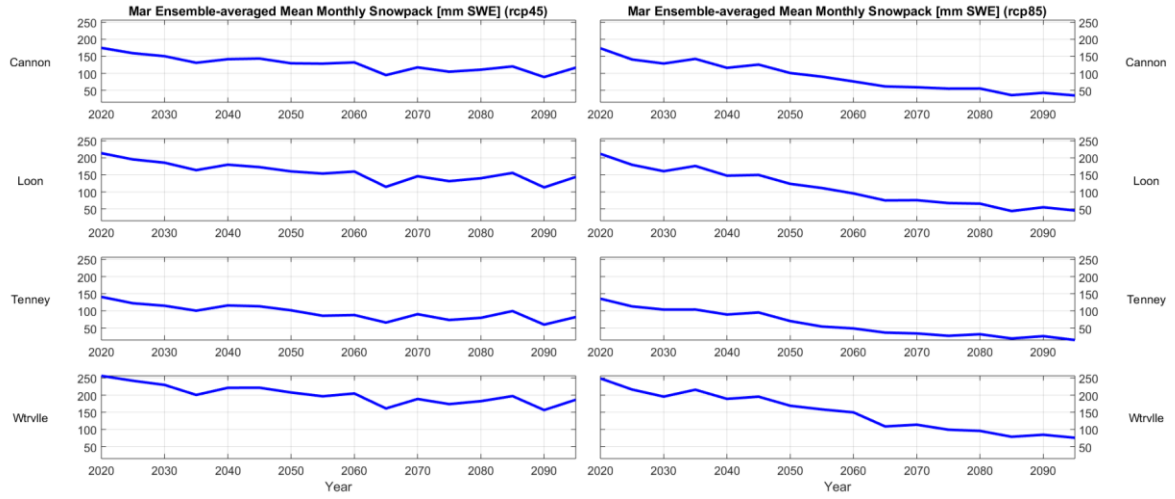

Fig. 2.5.3.: March ensemble-averaged mean monthly natural snowpack, 2020 – 2095.

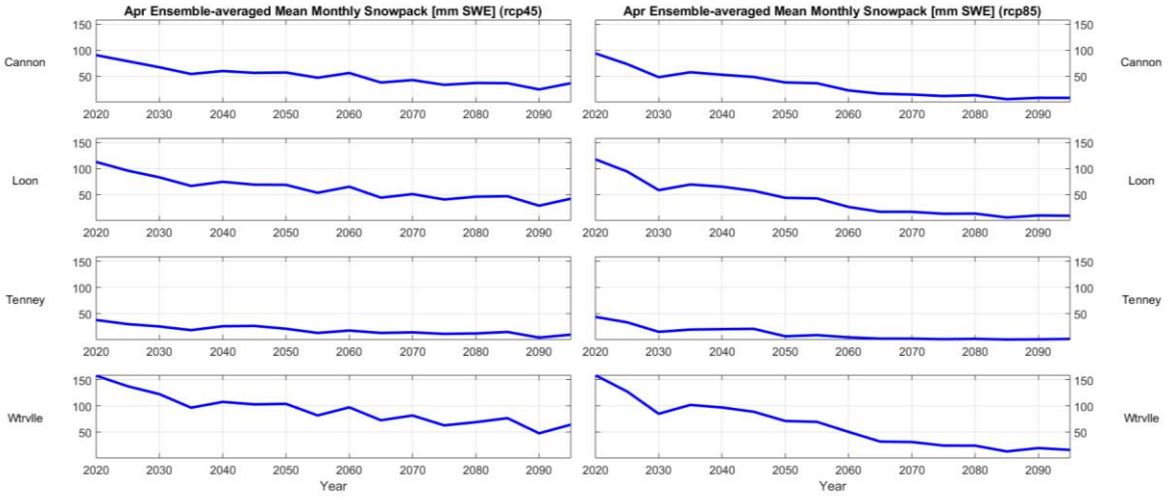

Fig. 2.5.4.: April ensemble-averaged mean monthly natural snowpack, 2020 – 2095.

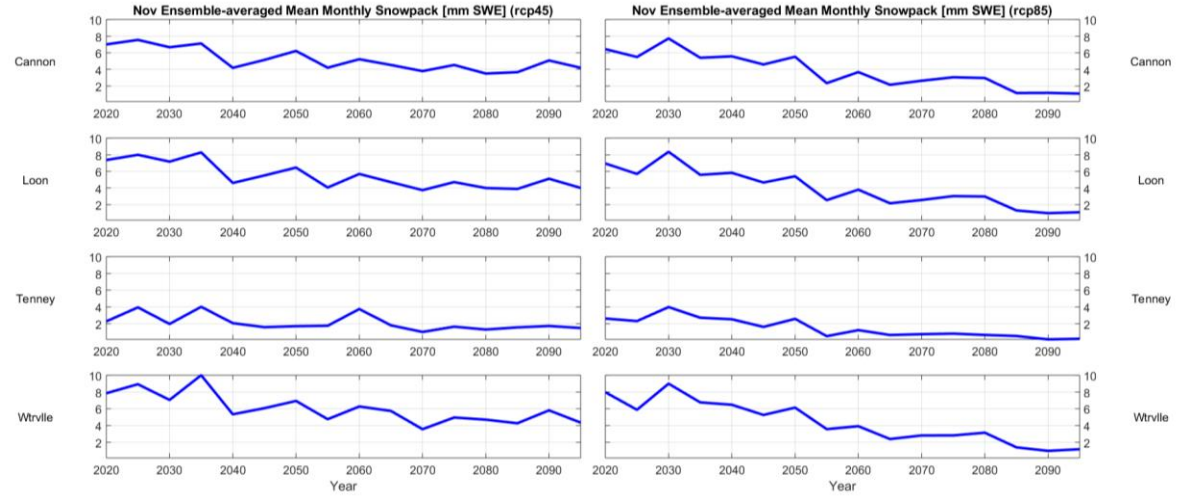

Fig. 2.5.5.: November ensemble-averaged mean monthly natural snowpack, 2020 – 2095.

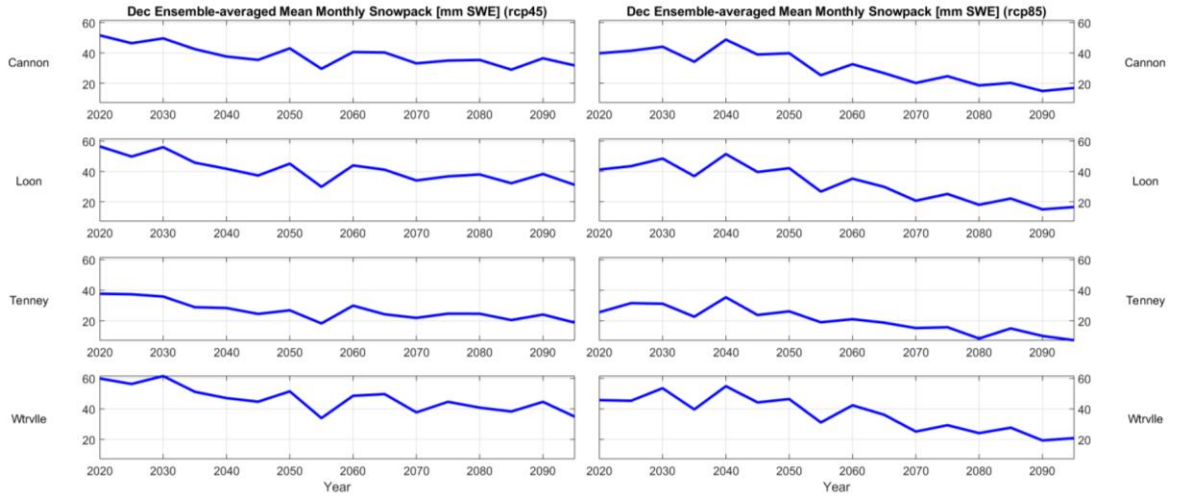

Fig. 2.5.6.: December ensemble-averaged mean monthly natural snowpack, 2020 – 2095.

Warm-Season Results. As with the cold-season results, two separate sets of results are shown, corresponding to the RCP4.5 and RCP8.5 emissions scenarios. These are presented here graphically. Interpretation is in Summary and Conclusions (below).

1. Number of days with maximum temperature ≥ 90 °F (32.2 °C):

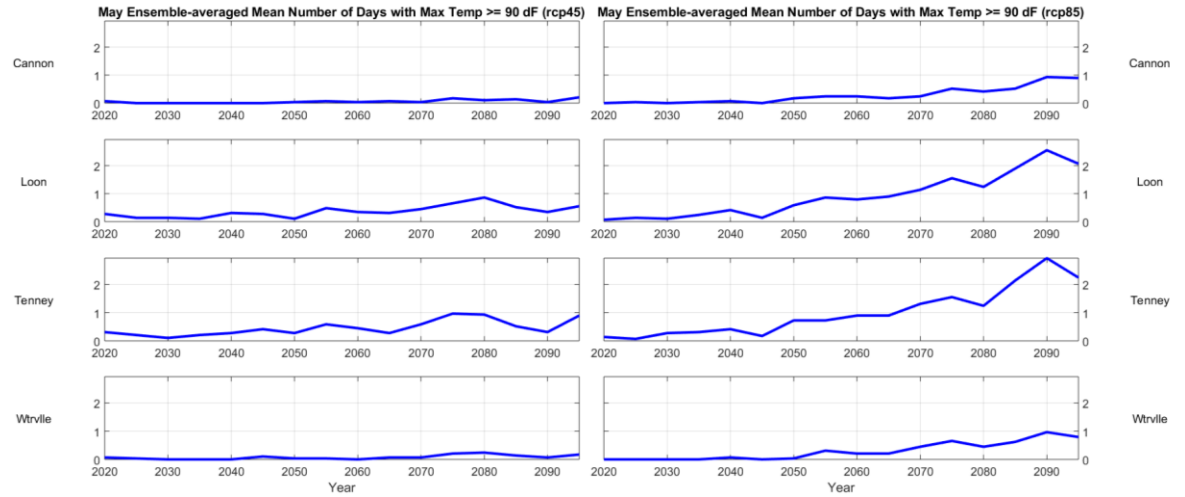

Fig. 3.1.1.: May ensemble-averaged number of days with maximum temperature ≥ 90 °F, 2020 – 2095. Left column corresponds to RCP4.5; right column to RCP8.5. Rows correspond to different locations. Horizontal axis is years; vertical axis is number of days during the month meeting or exceeding the threshold.

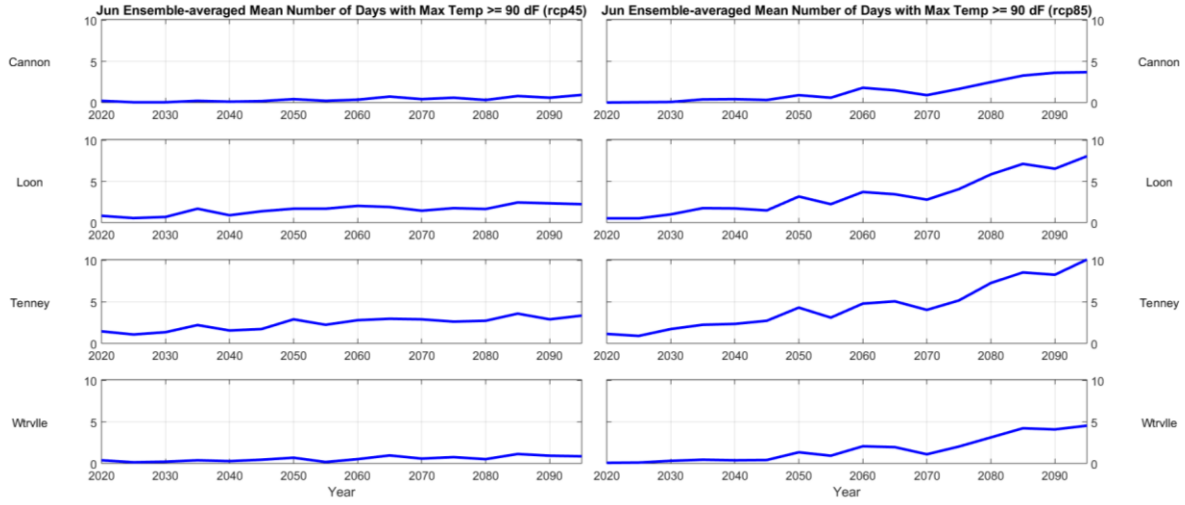

Fig. 3.1.2.: June ensemble-averaged number of days with maximum temperature ≥ 90 °F, 2020 – 2095.

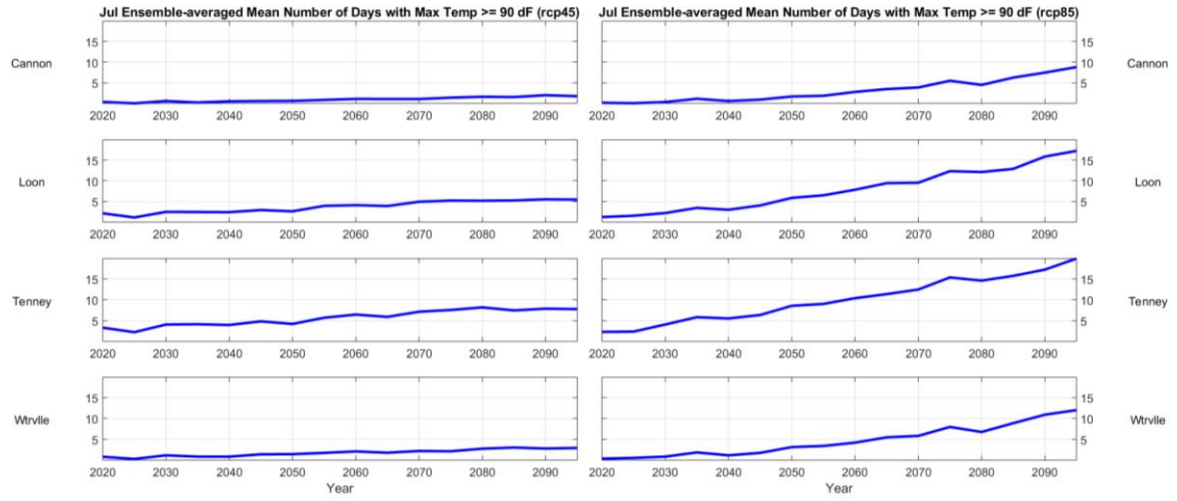

Fig. 3.1.3.: July ensemble-averaged number of days with maximum temperature ≥ 90 °F, 2020 – 2095.

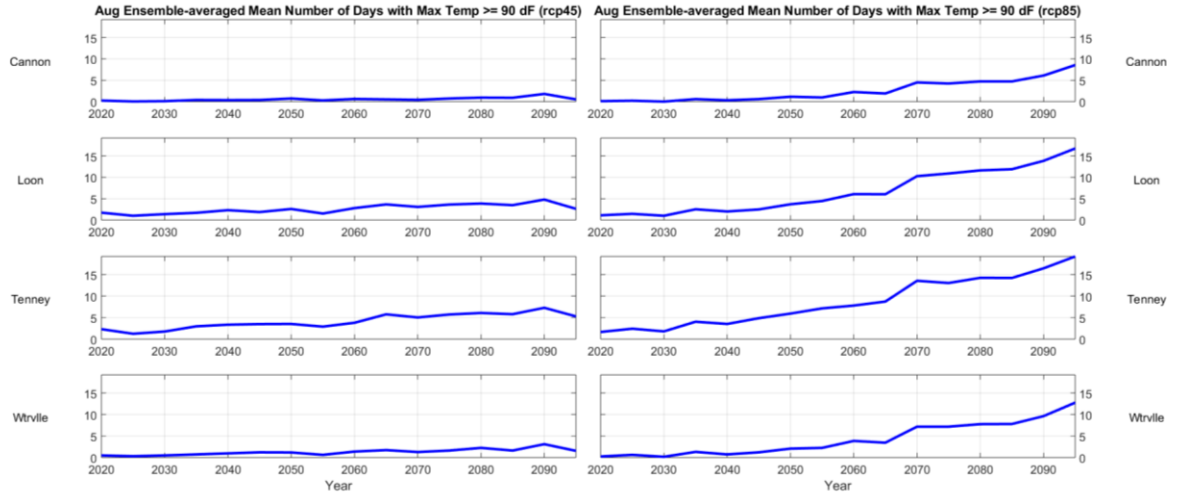

Fig. 3.1.4.: August ensemble-averaged number of days with maximum temperature ≥ 90 °F, 2020 – 2095.

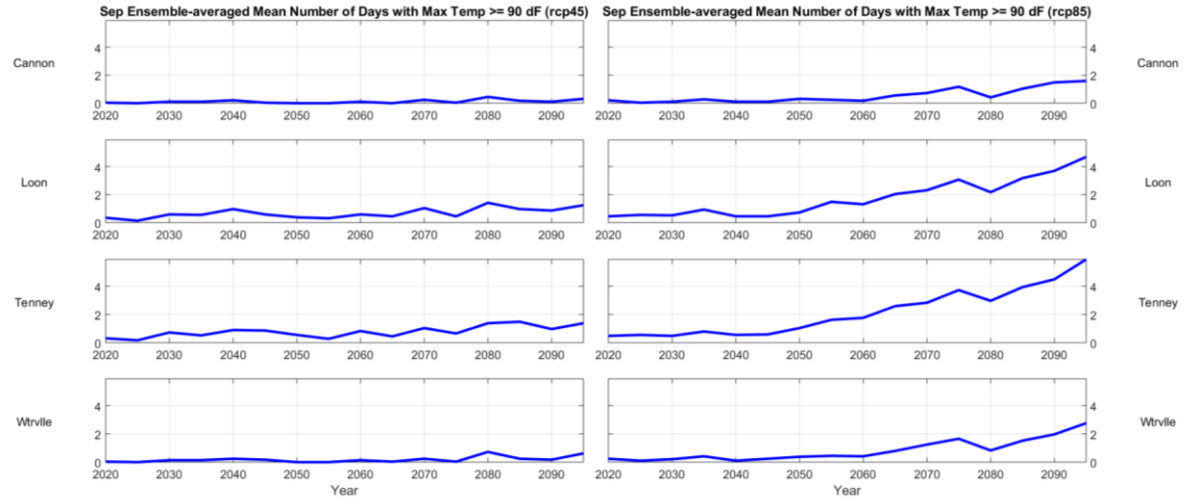

Fig. 3.1.5.: September ensemble-averaged number of days with maximum temperature ≥ 90 °F, 2020 – 2095.

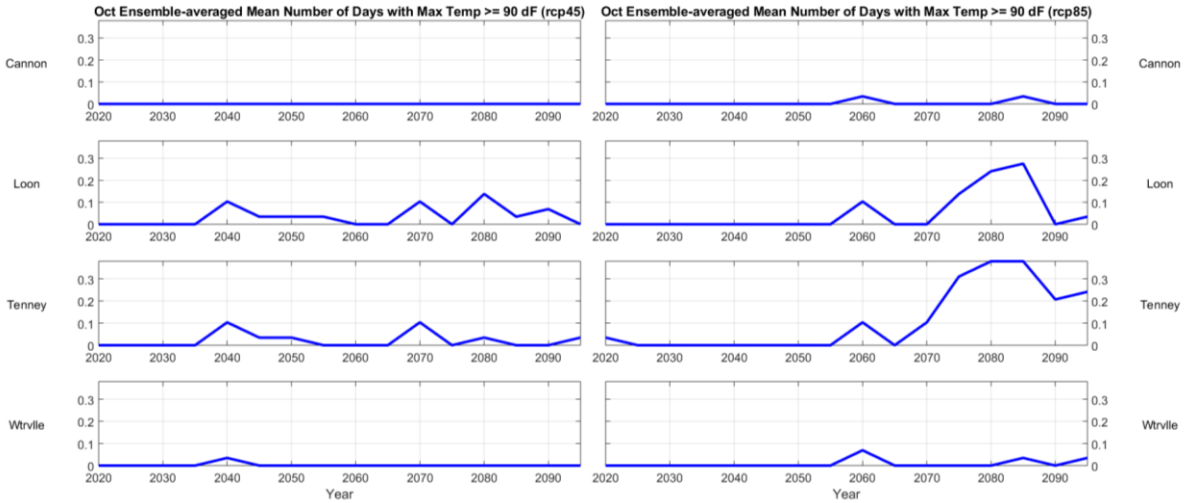

Fig. 3.1.6.: October ensemble-averaged number of days with maximum temperature ≥ 90 °F, 2020 – 2095.

2. Ensemble-average warm season precipitation; total by month:

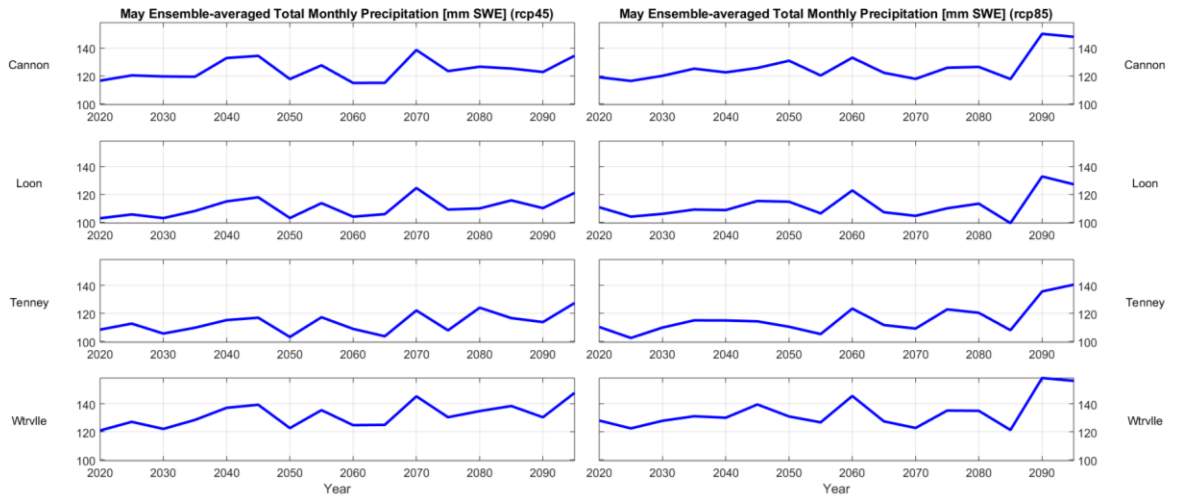

Fig. 3.2.1.: May ensemble-averaged total monthly precipitation, 2020 – 2095. Left column corresponds to RCP4.5; right column to RCP8.5. Rows correspond to different locations. Horizontal axis is years; vertical axis is total monthly precipitation [mm].

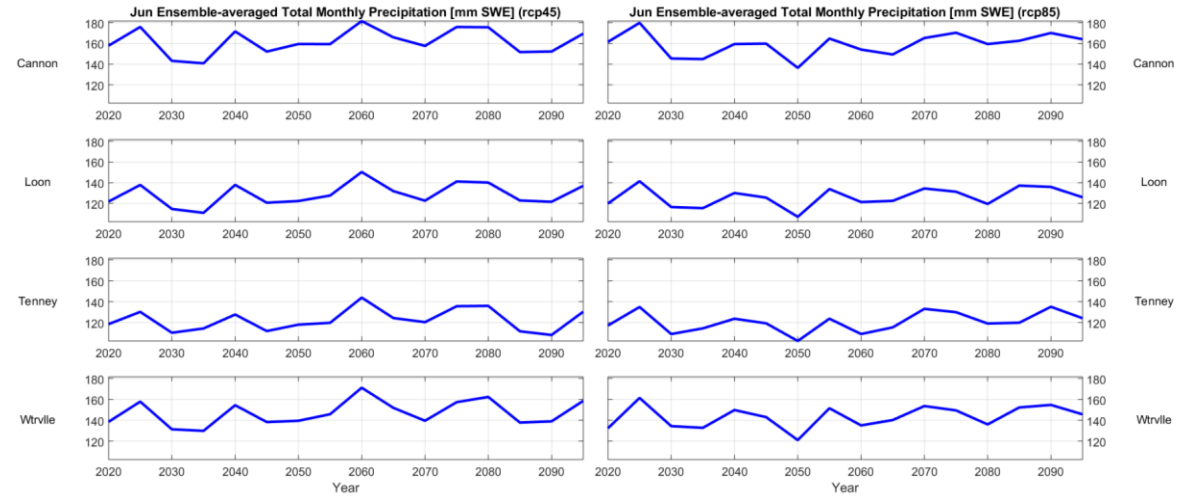

Fig. 3.2.2.: June ensemble-averaged total monthly precipitation, 2020 – 2095.

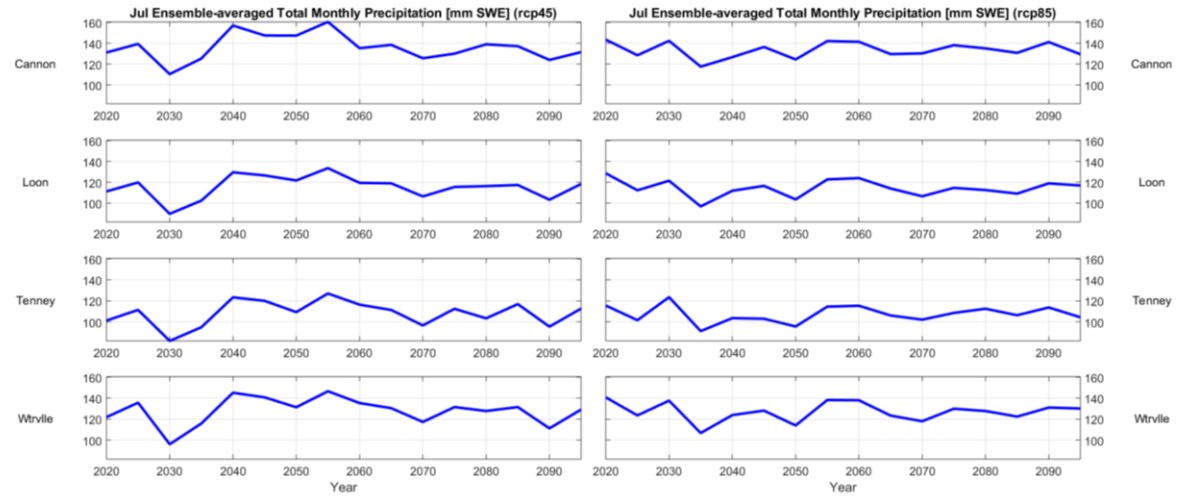

Fig. 3.2.3.: July ensemble-averaged total monthly precipitation, 2020 – 2095.

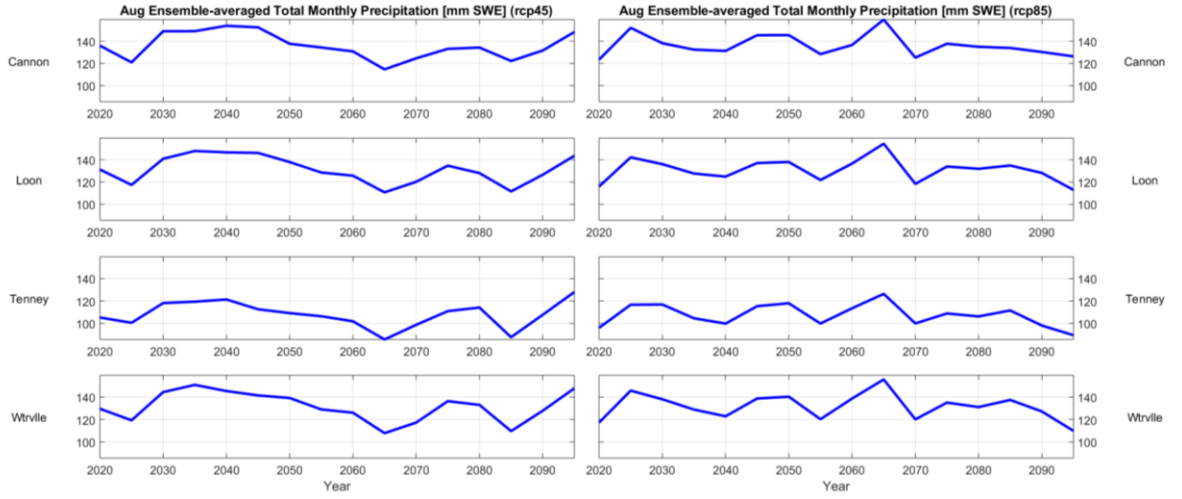

Fig. 3.2.4.: August ensemble-averaged total monthly precipitation, 2020 – 2095.

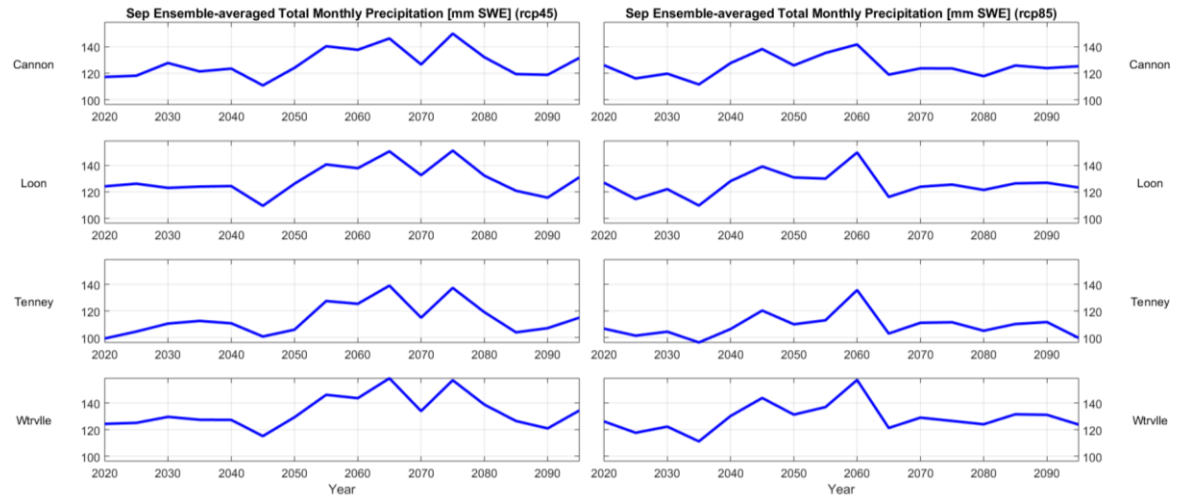

Fig. 3.2.5.: September ensemble-averaged total monthly precipitation, 2020 – 2095.

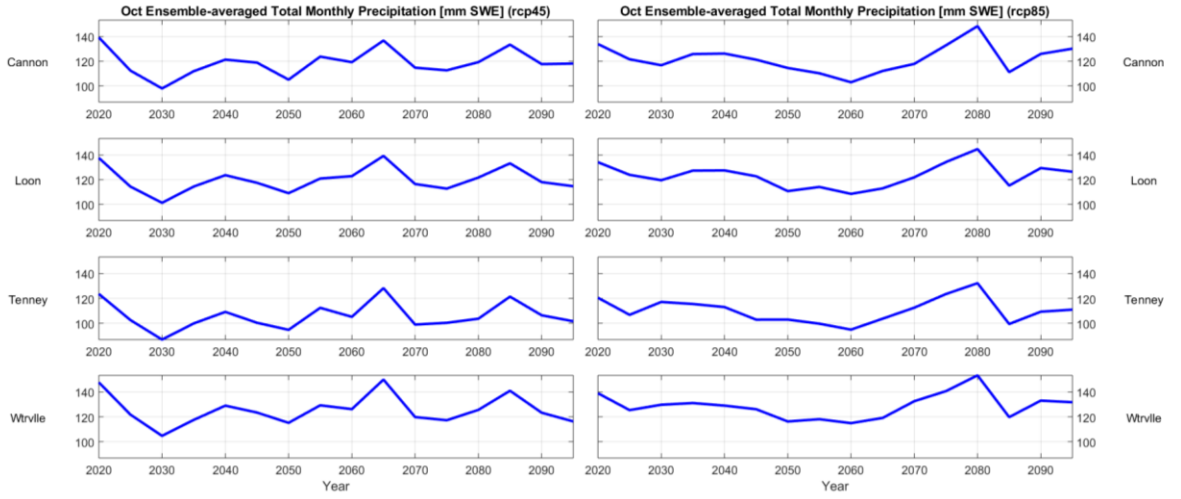

Fig. 3.2.6.: October ensemble-averaged total monthly precipitation, 2020 – 2095.

3. Ensemble-average number of warm-season zero-precipitation events ("droughts"), by number of days:

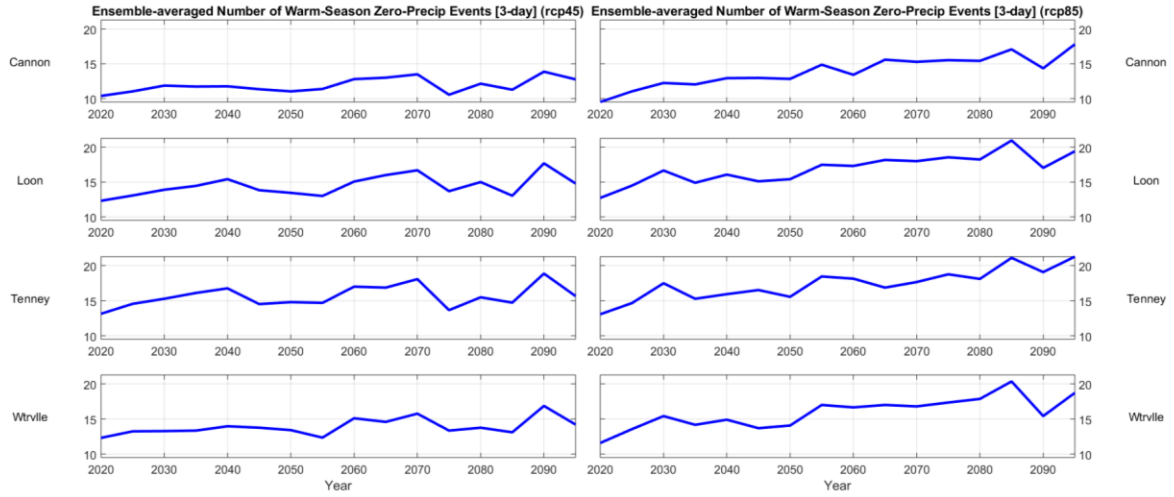

Fig. 3.3.1.: Ensemble-averaged number of warm-season 3-day zero-precipitation events, 2020 - 2095. Left column corresponds to RCP4.5; right column to RCP8.5. Rows correspond to different locations. Horizontal axis is years; vertical axis is number of individual events meeting the criteria.

Fig. 3.3.2.: Ensemble-averaged number of warm-season 5-day zero-precipitation events, 2020 - 2095.

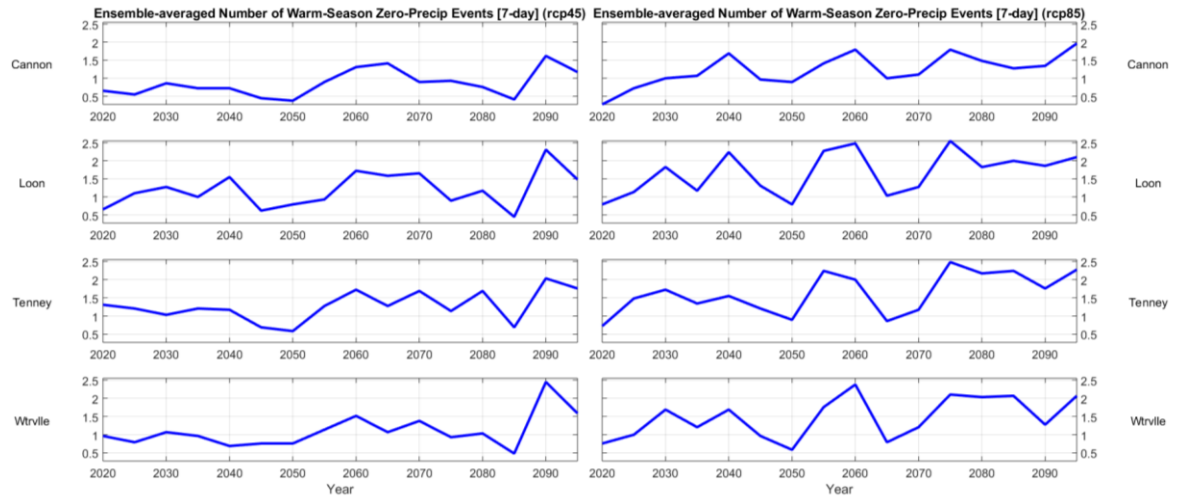

Fig. 3.3.3.: Ensemble-averaged number of warm-season 7-day zero-precipitation events, 2020 - 2095.

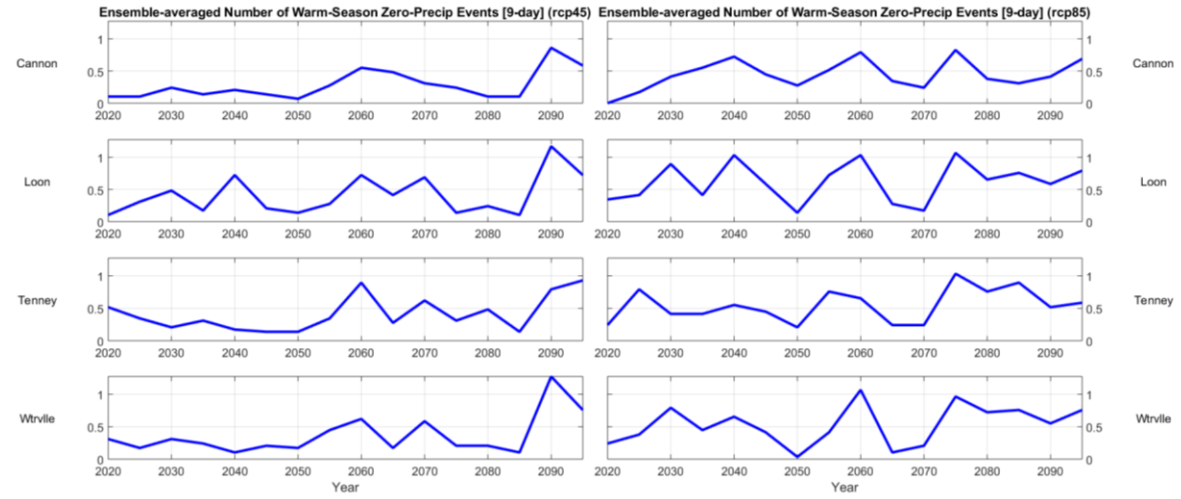

Fig. 3.3.4.: Ensemble-averaged number of warm-season 9-day zero-precipitation events, 2020 - 2095.

Fig. 3.3.5.: Ensemble-averaged number of warm-season 11-day zero-precipitation events, 2020 - 2095.

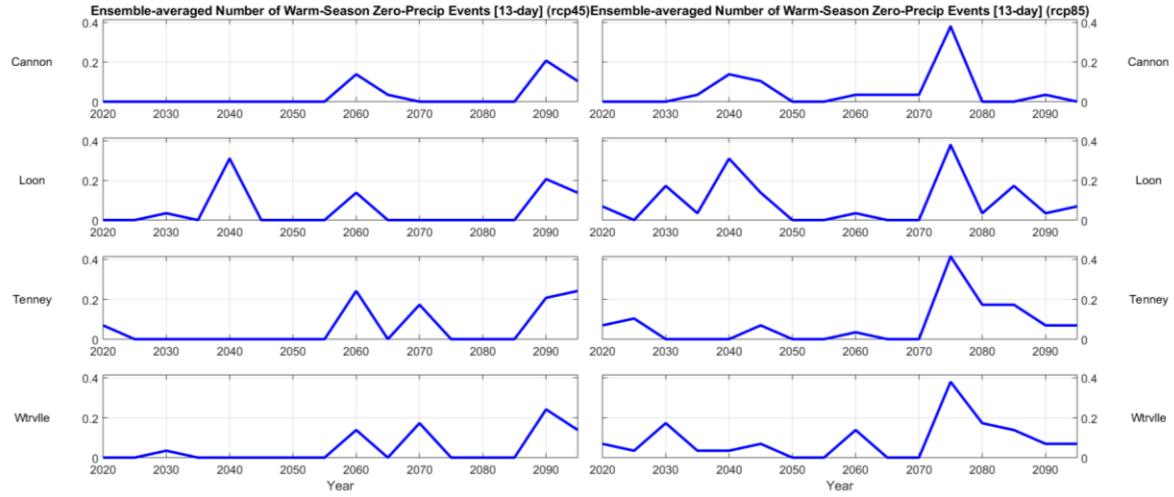

Fig. 3.3.6.: Ensemble-averaged number of warm-season 13-day zero-precipitation events, 2020 - 2095.

Fig. 3.3.7.: Ensemble-averaged number of warm-season 15-day zero-precipitation events, 2020 - 2095.

4. Ensemble average number of warm-season daily precipitation events in category:

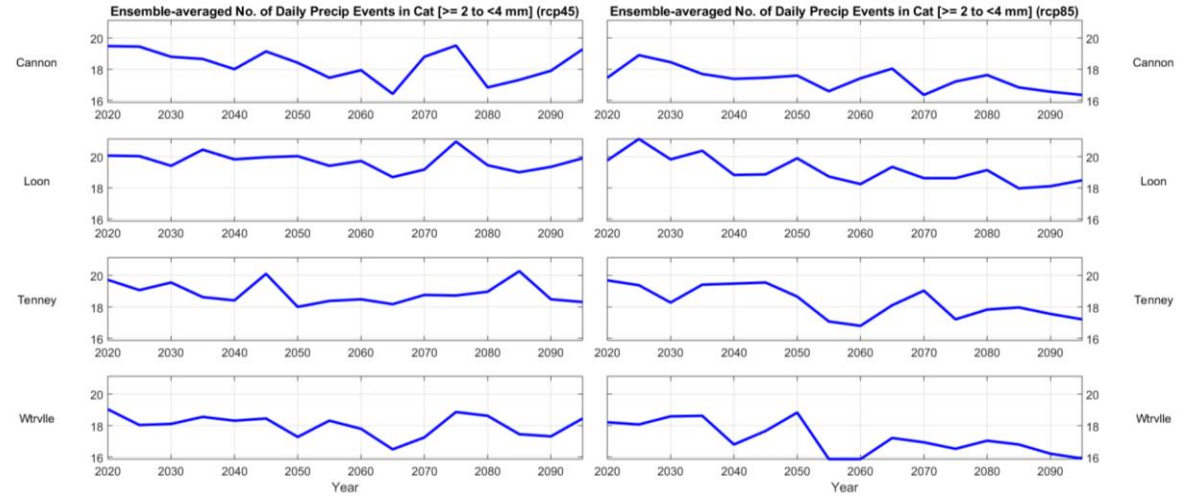

Fig. 3.4.1.: Ensemble-averaged number of warm-season precipitation events ≥ 2 to < 4 mm, 2020 - 2095. Left column corresponds to RCP4.5; right column to RCP8.5. Rows correspond to different locations. Horizontal axis is years; vertical axis is number of individual events meeting the criteria.

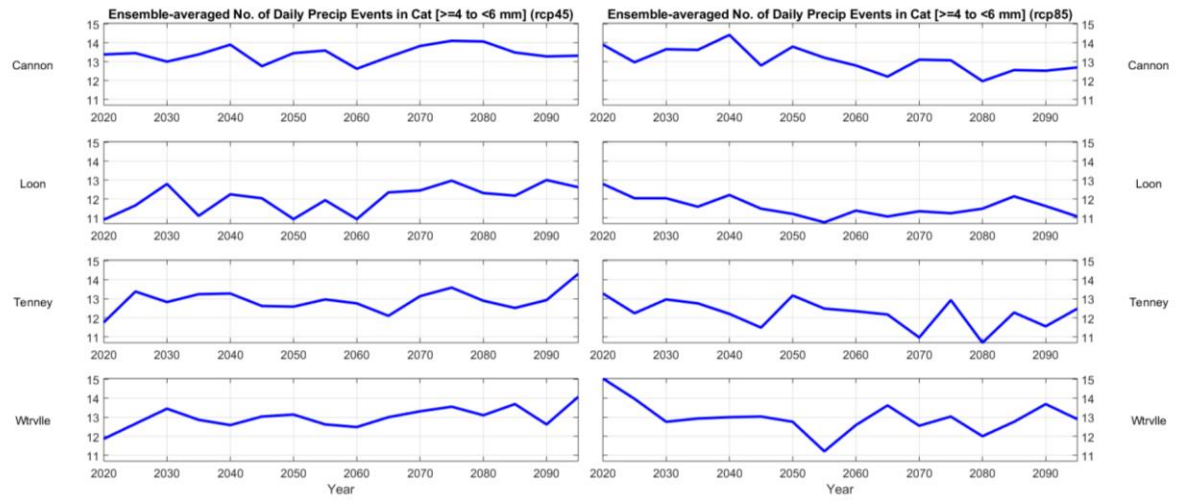

Fig. 3.4.2.: Ensemble-averaged number of warm-season precipitation events ≥ 4 to < 6 mm, 2020 - 2095.

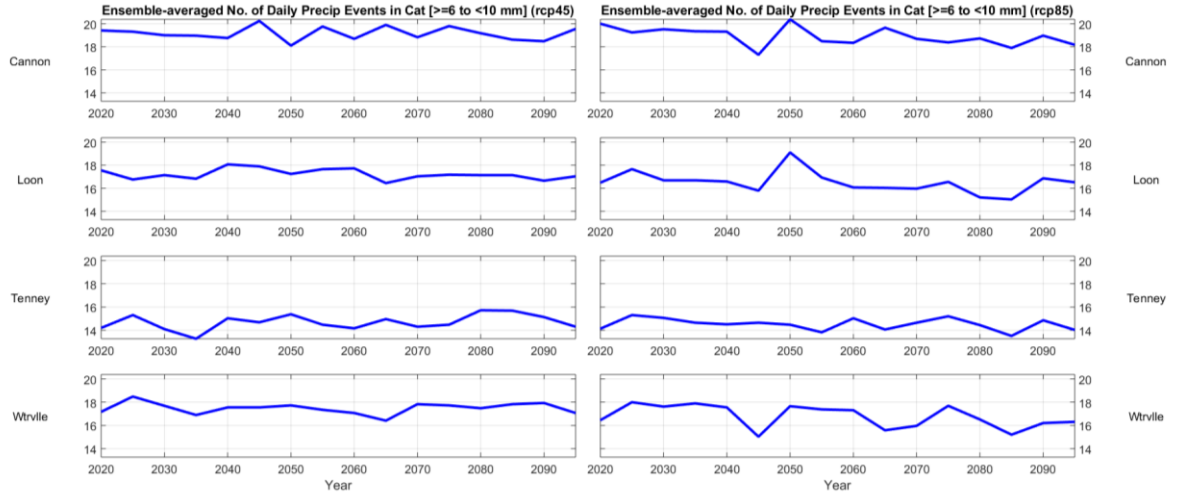

Fig. 3.4.3.: Ensemble-averaged number of warm-season precipitation events ≥ 6 to < 10 mm, 2020 - 2095.

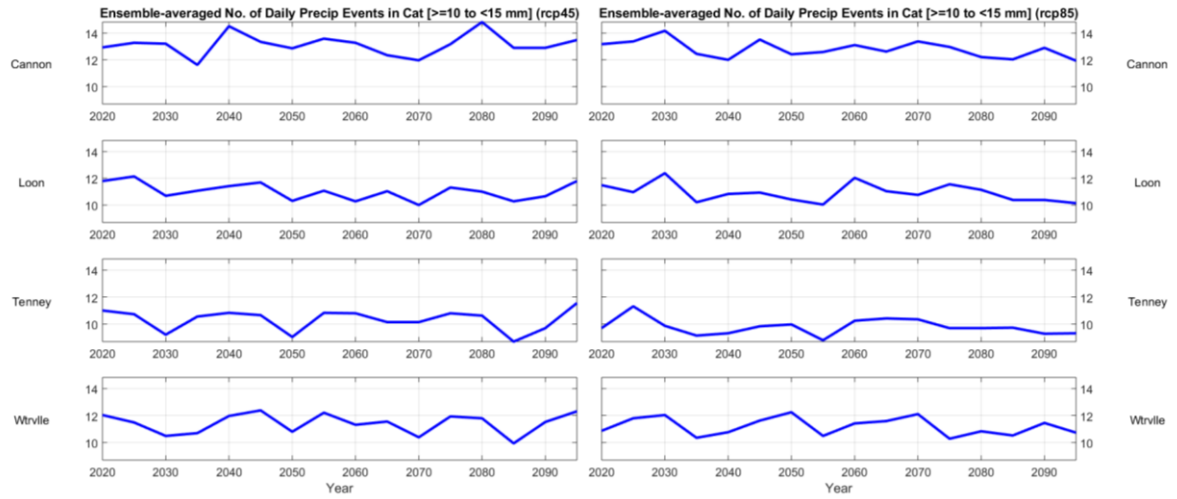

Fig. 3.4.4.: Ensemble-averaged number of warm-season precipitation events ≥ 10 to < 15 mm, 2020 - 2095.

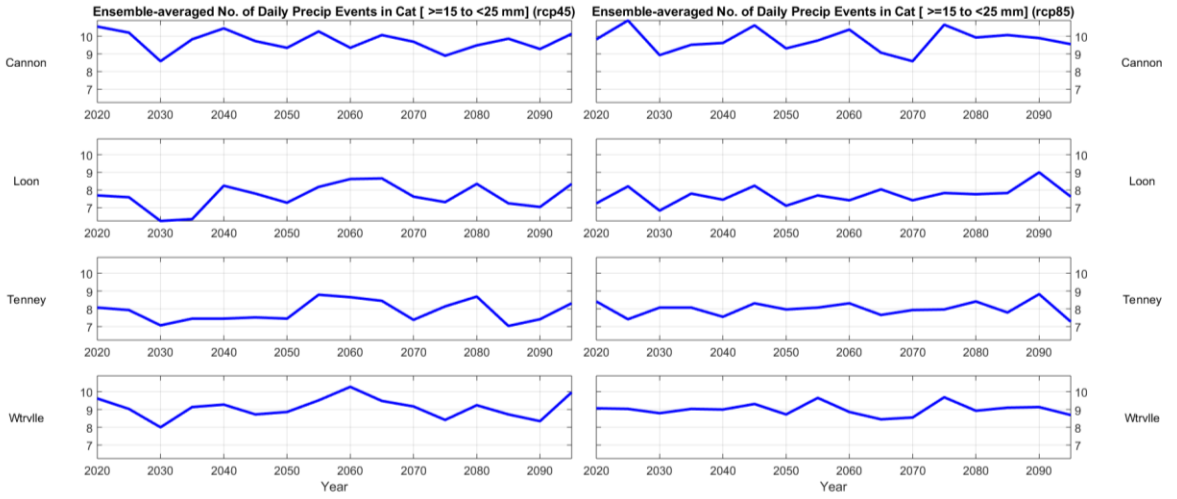

Fig. 3.4.5.: Ensemble-averaged number of warm-season precipitation events ≥ 15 to < 25 mm, 2020 - 2095.

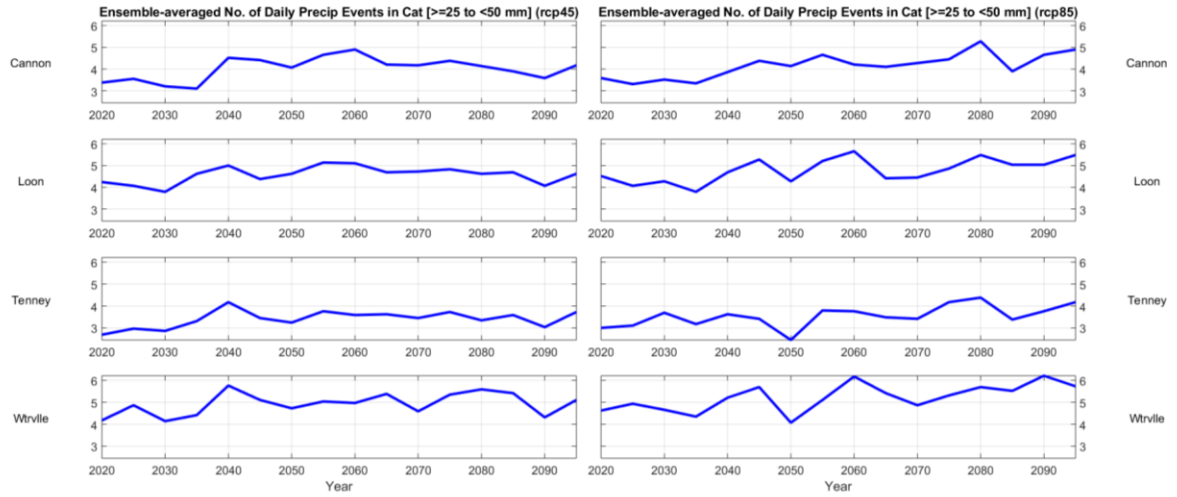

Fig. 3.4.6.: Ensemble-averaged number of warm-season precipitation events ≥ 25 to < 50 mm, 2020 - 2095.

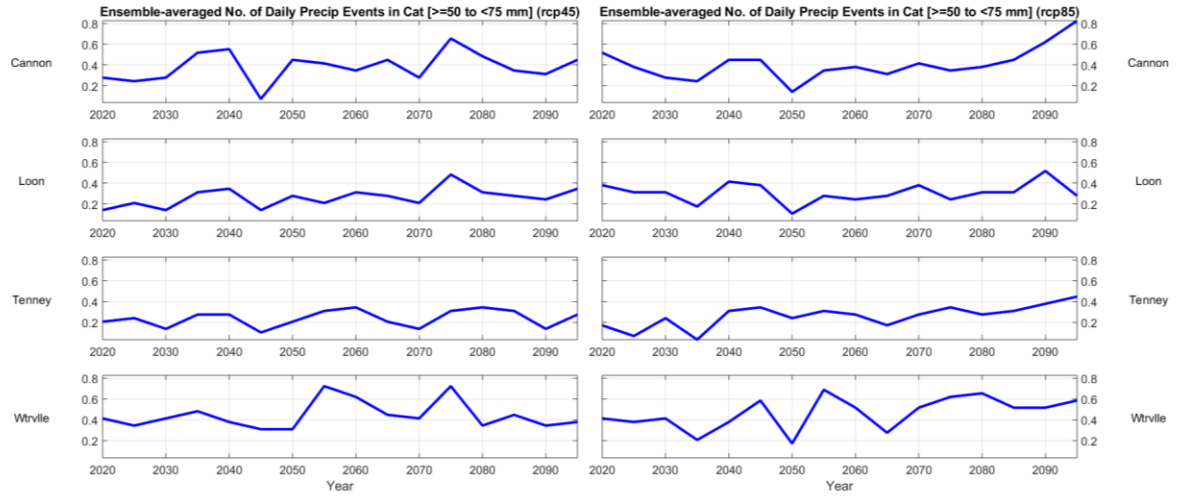

Fig. 3.4.7.: Ensemble-averaged number of warm-season precipitation events ≥ 50 to < 75 mm, 2020 - 2095.

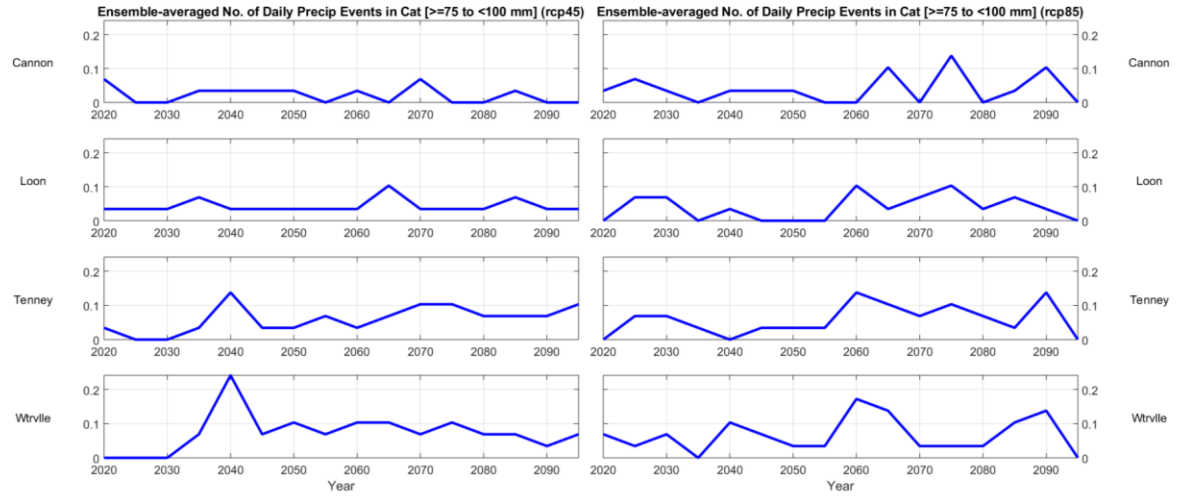

Fig. 3.4.8.: Ensemble-averaged number of warm-season precipitation events ≥ 75 to < 100 mm, 2020 - 2095.

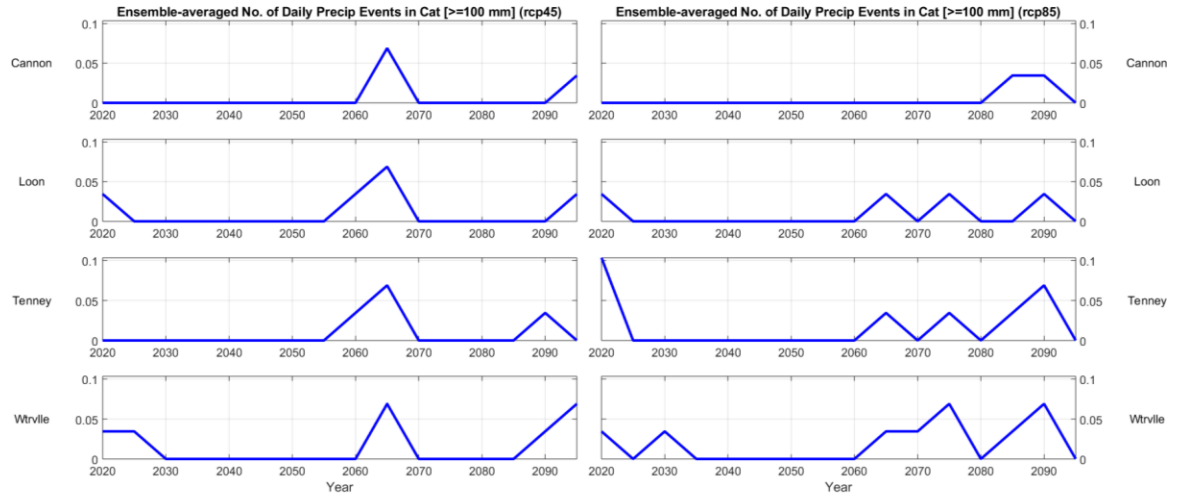

Fig. 3.4.9.: Ensemble-averaged number of warm-season precipitation events ≥ 100 mm, 2020 - 2095.

5. Ensemble average number of warm-season daily precipitation events in category, with improved mid-range resolution:

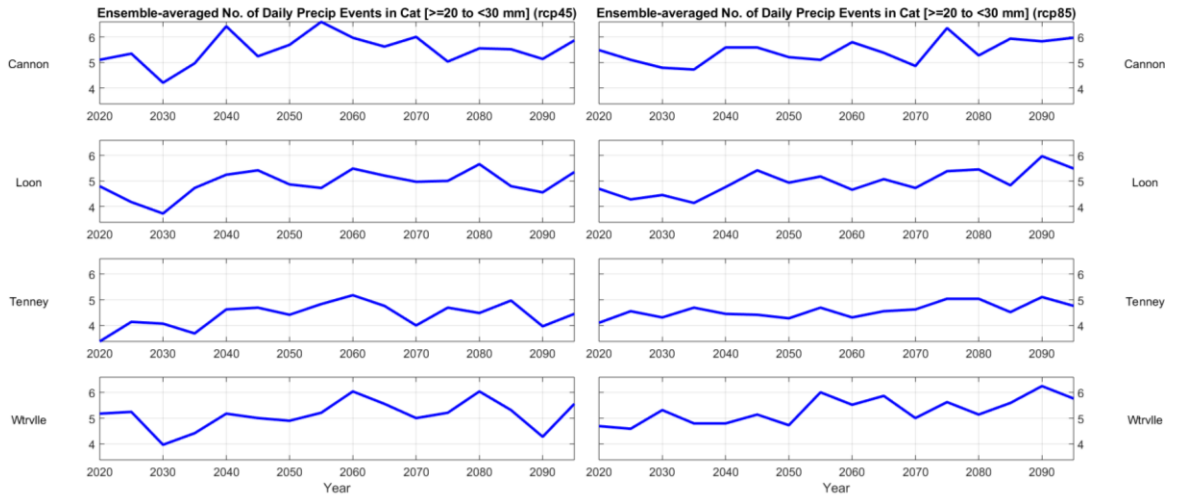

Fig. 3.5.1.: Ensemble-averaged number of warm-season precipitation events ≥ 20 to < 30 mm, 2020 - 2095. Left column corresponds to RCP4.5; right column to RCP8.5. Rows correspond to different locations. Horizontal axis is years; vertical axis is number of individual events meeting the criteria.

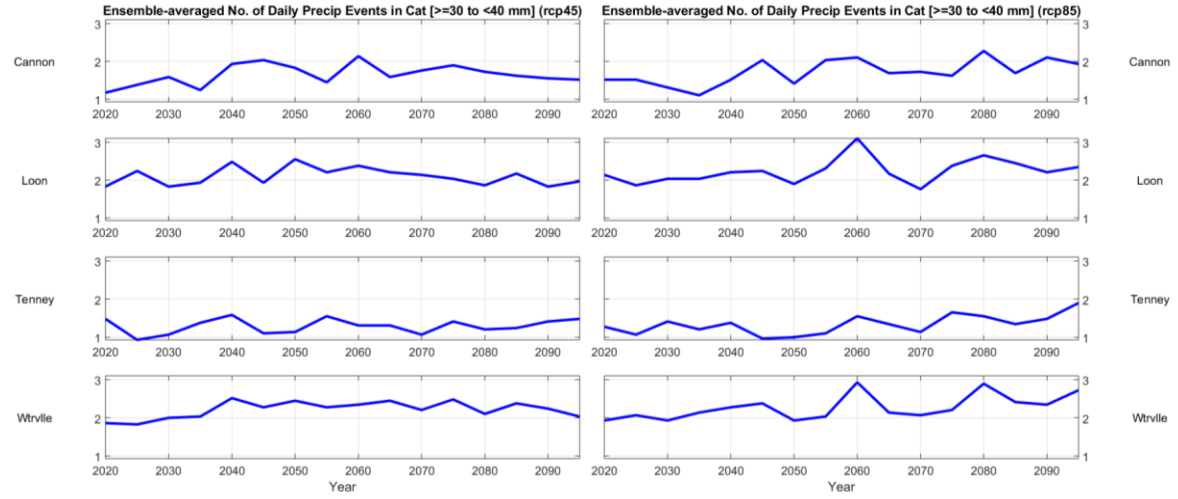

Fig. 3.5.2.: Ensemble-averaged number of warm-season precipitation events ≥ 30 to < 40 mm, 2020 - 2095.

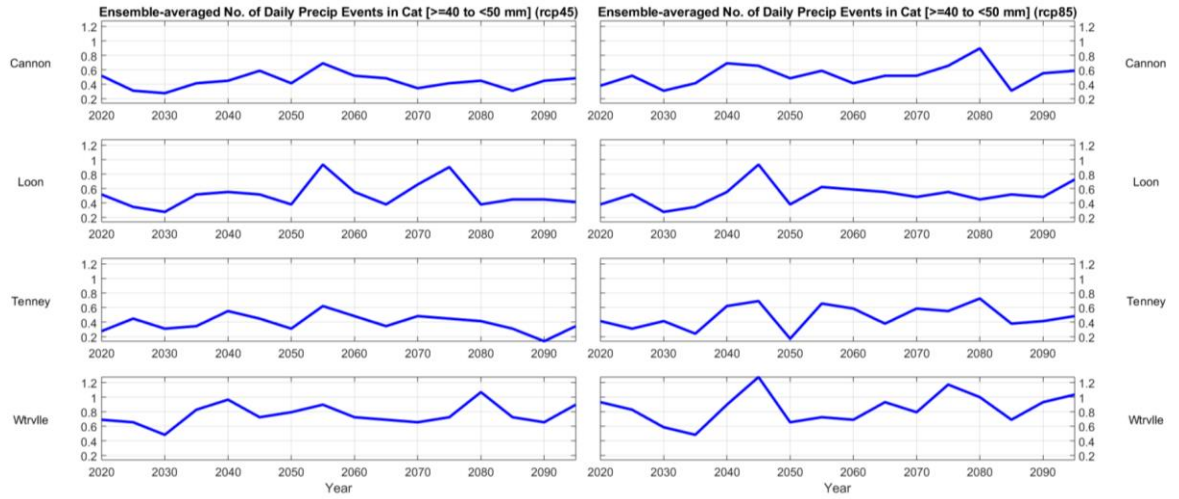

Fig. 3.5.3.: Ensemble-averaged number of warm-season precipitation events ≥ 40 to < 50 mm, 2020 - 2095.

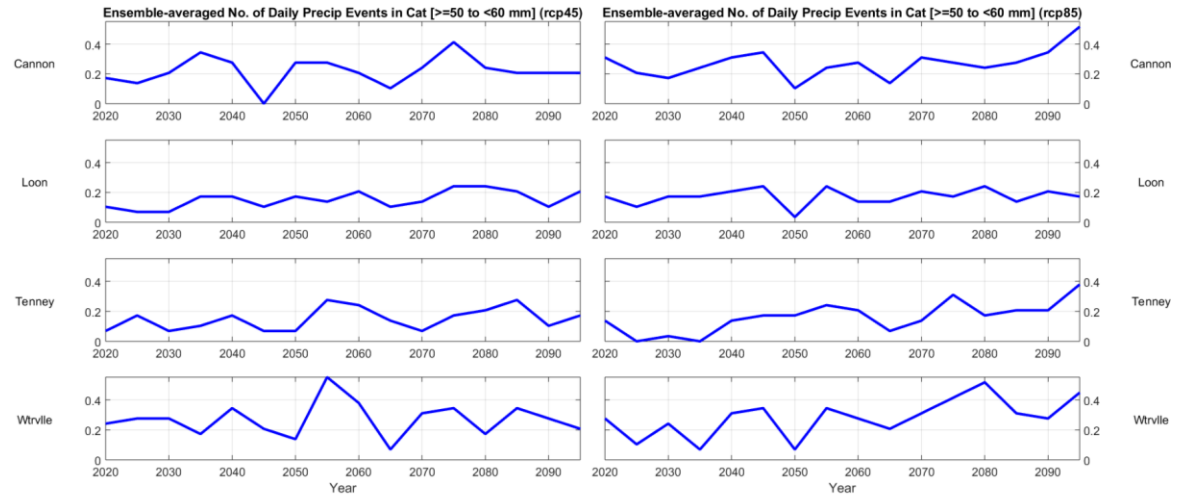

Fig. 3.5.4.: Ensemble-averaged number of warm-season precipitation events ≥ 50 to < 60 mm, 2020 - 2095.

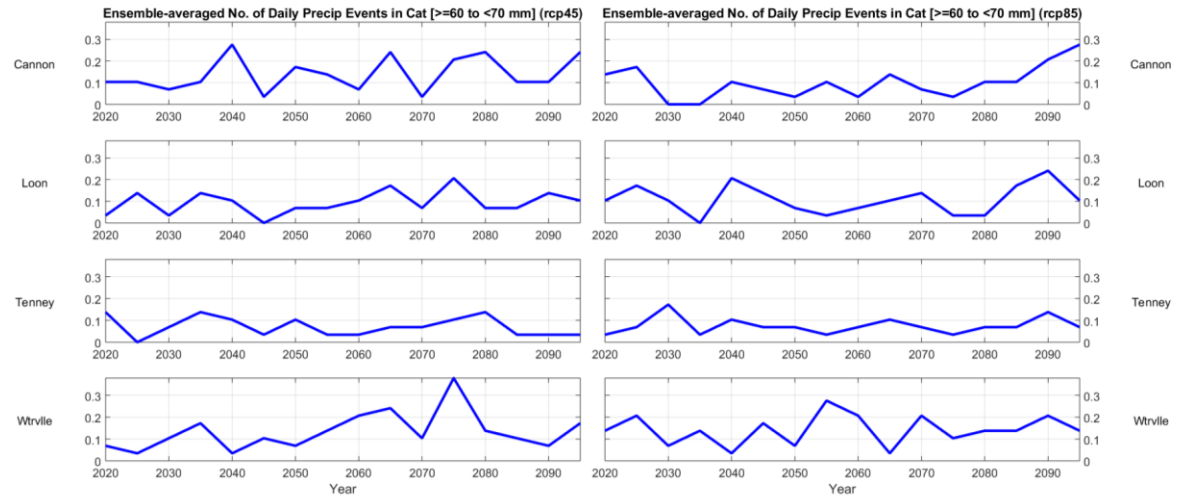

Fig. 3.5.5.: Ensemble-averaged number of warm-season precipitation events ≥ 60 to < 70 mm, 2020 - 2095.

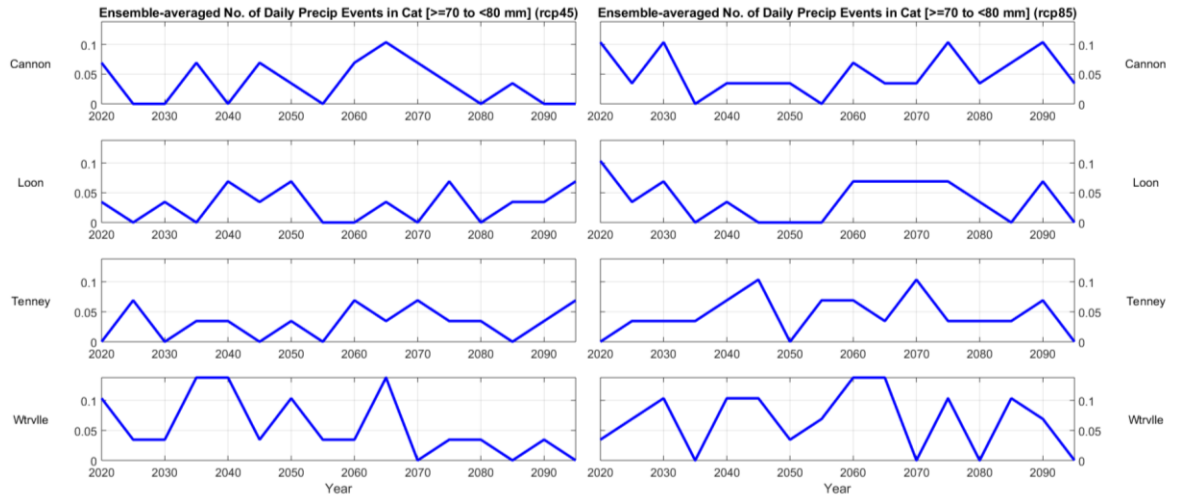

Fig. 3.5.6.: Ensemble-averaged number of warm-season precipitation events ≥ 70 to < 80 mm, 2020 - 2095.

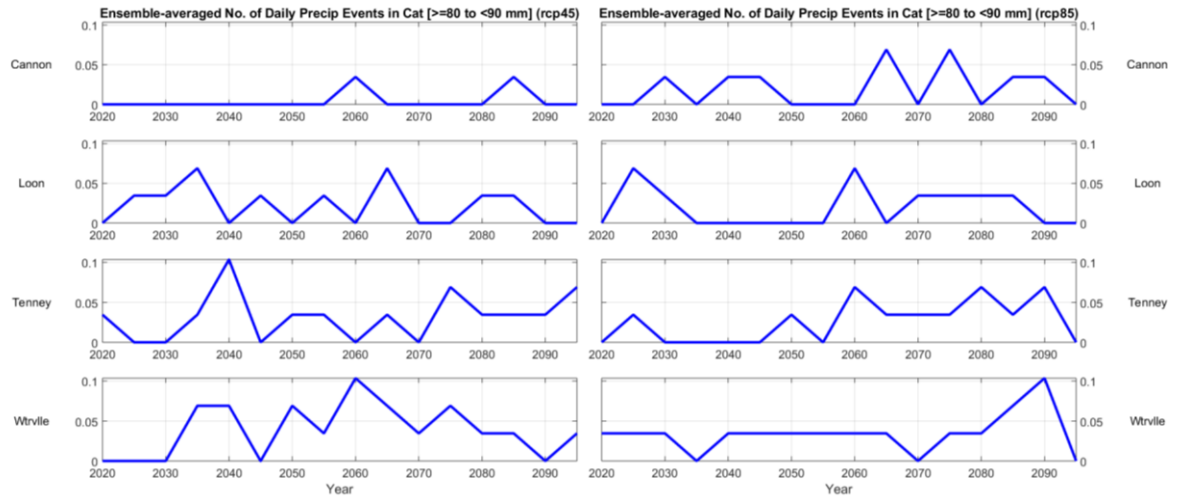

Fig. 3.5.7.: Ensemble-averaged number of warm-season precipitation events ≥ 80 to < 90 mm, 2020 - 2095.

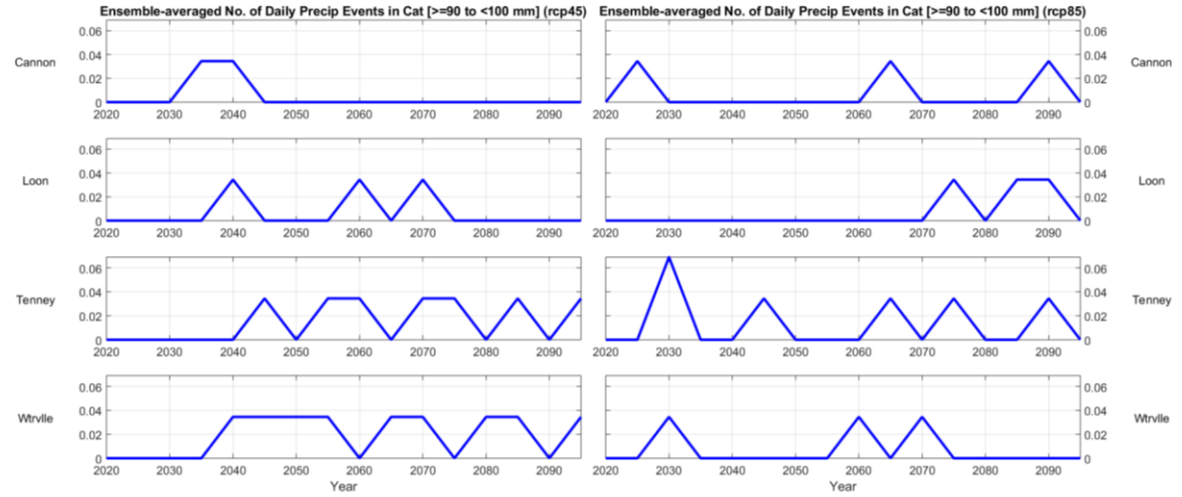

Fig. 3.5.8.: Ensemble-averaged number of warm-season precipitation events ≥ 90 to < 100 mm, 2020 - 2095.

Description of Results.

1. **Cold-season.**

1.1. **Minimum daily temperatures.** As stated in Part 1 of the Physical Sciences Report, changes in minimum daily temperature during the period 2020 – 2040 are relatively insensitive to RCP. In both cases, and across all six months of the cold season, the ensemble indicates increases in mean monthly minimum temperature (MMMT) at all locations on the order of 1 – 2 °C (2 – 4 °F). However the RCP-dependent differences become evident by about mid-century, and quite significant by 2095.

- In January (Fig. 2.1.1), RCP4.5 is associated with an increase in MMMT of about 3 °C (5 °F), while RCP8.5 indicates increase of 6 – 7 °C (11 – 13 °F) by the end of the century.

- In February and March (Figs. 2.1.2 and 2.1.3), RCP4.5 is associated with an increase of 2 °C (4 °F), while RCP8.5 is associated with an increase of about 6 °C (11 °F).

- In April (Fig. 2.1.4), RCP4.5 results in MMMT exceeding the freezing point of water at Cannon and Loon by 2050, at Tenney Mountain by 2060, and at Waterville Valley by about 2070. RCP8.5 results in MMMT at *all* locations exceeding 0 °C (32 °F) by 2060.

- In November (Fig. 2.1.5), MMMT increases by 2 - 3 °C (4 – 5 °F) by 2095 with RCP4.5, and by about 5 °C (9 °F) with RCP8.5. With RCP8.5, MMMT exceeds the freezing point of water at three of the four locations by about 2080.

- December (Fig. 2.1.6) MMMTs increases by 2 – 3 °C (4 – 5 °F) with RCP4.5 by 2095, and 4 – 5 °C (7 – 9 °F) with RCP8.5, although, in both cases, they remain below the freezing point of water.

1.2. **Number of days when snowmaking is possible.** During the period 2020 – 2040, there is relatively little difference between RCP4.5 and RCP8.5. More dramatic changes emerge at three of the four locations by mid-century.

- In January (Fig. 2.2.1), RCP4.5 is associated with a decrease in the number of days ranging from zero (at Waterville Valley) to about three (at Cannon). RCP8.5 shows larger decreases, ranging from two fewer days (at Waterville Valley) to four fewer days (at Loon). There is a similar distribution of results for February (Fig. 2.2.2).

- March (Fig. 2.2.3) shows larger decreases with both RCPs. With RCP4.5, there is a range from one fewer day (at Cannon) to two fewer days (at Loon and Tenney Mountain). With RCP8.5, decreases range from 6 – 7 fewer viable days, depending on location.

- April's (Fig. 2.2.4) pattern is stronger than March's. RCP4.5 shows a decrease of about 3 – 4 viable days by 2040, and 5 – 6 fewer viable days by 2095. RCP8.5 shows similar reductions by 2040, but by 2095 the reduction grows to 8 – 15 viable days, depending on location (resulting in between about 5 and 9 viable days remaining by the end of the century).

- In November (Fig. 2.2.5), RCP4.5 is associated with a loss of about three viable days by 2040, and 5 – 6 days 2095. RCP8.5 is associated with a loss of about 11 – 13 days, depending on location (resulting in between about 7 and 13 days by the end of the century).

- In December (Fig. 2.2.6), RCP4.5 is associated with a loss of 1 – 2 days by 2040, and 2 – 4 days by 2095. RCP8.5 is associated with no loss of snowmaking days by 2040, but reductions of 3 – 6 days by 2095 (reducing the total to between 21 and 27 days by the end of the century).

1.3. **Total monthly snowfall.** Here, location-dependent differences emerge between the two RCPs.

- In January (Fig. 2.3.1), RCP4.5 is associated with fluctuating snowfall amounts during the 21st Century, but there are no important changes between the present 2020 and 2095. RCP8.5 is not associated with any important changes between 2020 and 2040, but shows reductions in total snowfall of between zero (at Waterville Valley) and about 20 mm (about 0.8 inches) SWE (at

Tenney Mountain). With RCP8.5, snowfall totals fall to between and 50 mm (2.0 inch) SWE and 80 mm (3.2 inch) SWE by the end of the century.

- February's (Fig. 2.3.2) results are similar to January's, except that reductions in total snowfall of between 20 and 30 mm (0.8 to 1.2 inches) SWE appear at all four locations with RCP8.5. By 2095, RCP8.5 is associated with snowfall totals of between about 30 and about 55 mm (1.2 to 2.2 inches) SWE.

- March (Fig. 2.3.3) shows reductions at all four locations with both RCPs by 2040. By 2095, RCP4.5 is associated with a reduction of 10 – 20 mm (0.4 to 0.8 inches) SWE at all locations, while RCP8.5 is associated with reductions of 30 – 50 mm (1.2 to 2.0 inches) SWE. Snowfall totals range from about 20 mm (0.8 inch) SWE to just less than 40 mm (1.6 inch) SWE.

- April (Fig. 2.3.4) is similar to March, with both RCPs showing reductions of 5 – 15 mm (0.2 to 0.6 inches) by 2040. RCP4.5 is associated with a mid-century *increase* back to levels near those of 2020, but this is not evident with RCP8.5. By the end of the century, RCP4.5 is associated with a reduction of 5 – 15 mm, while RCP8.5 is associated with reductions of 5 – 12 mm (0.2 to 0.5 inches). Further, with RCP8.5, total monthly snowfall amounts are essentially zero by 2095.

- In November (Fig. 2.3.5), RCP4.5 is associated with either zero or very small reductions in snowfall by 2040, and reductions of 10 – 15 mm (0.4 to 0.6 inches) SWE by 2095. RCP8.5 is associated with reductions of 8 – 10 mm (0.3 to 0.4 inches) by 2040, and 10 – 35 mm (0.4 to 1.4 inches) SWE by 2095. One location (Tenney Mountain) shows zero natural snowfall remaining by 2095, and the remainder all show totals below 10 mm (0.4 inch) SWE.

- In December (Fig. 2.3.6), both RCPs are associated with a reduction of about 30 mm (1.2 inch) SWE at all four locations by 2040. By 2095, RCP4.5 is associated with a decrease of about 40 mm (1.6 inch) SWE, while RCP8.5 is associated with a decreases of 30 – 50 mm (1.2 to 2.0 inches), depending on location. With RCP8.5, end-of-century snowfall totals for the month range from about 40 mm (1.6 inch) to about 70 mm (2.8 inch) SWE, which is roughly half of 2020 values.

1.4. **Snowfall-to-precipitation ratio.** This parameter is relatively insensitive to RCP between 2020 and 2040, but important differences emerge by the end of the 21st Century.

- In January (Fig. 2.4.1), RCP4.5 and RCP8.5 are both associated with relatively small changes in this ratio. With RCP4.5, there is a reduction of about 10 percent at all locations by 2095. With RCP8.5., there is reduction of about 30 percent at all locations by 2095, with three (Cannon, Loon, and Tenney Mountain) all indicating that less than half of the total monthly precipitation will fall as snow, while Waterville Valley falls to just less than 60 percent.

- In February (Fig. 2.4.2), RCP4.5 and RCP8.5 both indicate little change by 2040. With RCP4.5, there is a reduction on the order of about 10 percent at all locations by 2095. With RCP8.5, there is a reduction of 20 – 40 percent by 2095, with three locations (Cannon, Loon, and Tenney Mountain) all indicating a ratio of less than 40 percent, and Waterville Valley indicating a ratio of slightly less than 50 percent.

- In March (Fig. 2.4.3), RCP4.5 is associated with little reduction in this ratio by 2040, while RCP8.5 is associated with a reduction of roughly 10 percent. By 2095, RCP4.5 indicates a reduction of

about 10 percent at all locations, while RCP8.5 indicates a reduction of 20 – 40 percent. RCP8.5 is associated with ratios of only about 20 percent by the end of the century.

- April (Fig. 2.4.4), which at present is the end of the ski season in New Hampshire, shows similar reductions, except they show up earlier, especially with RCP4.5. By 2040, RCP4.5 is associated with a reduction on the order of 10 percent, while RCP8.5 shows zero change to a slight increase, depending on location. By 2095, RCP4.5 shows the ratio dropping to between 5 and 10 percent, while RCP8.5 shows the ratio dropping to near zero. This result indicates that April will no longer be a skiing month in the Campton area by the end of the century, as almost all precipitation will fall in some form other than snow.

- In November (Fig. 2.4.5), RCP4.5 is not associated with any important changes to the ratio by 2040, while RCP8.5 is associated with decreases of about 10 percent at all locations. By 2095, RCP4.5 is associated with reductions of about 5 percent, while RCP8.5 is associated with reductions of about 20 percent at all locations. One location (Tenney Mountain) indicates a ratio near zero by the end of the century, while the other three are all below 10 percent by that time. This result indicates that, like April, November will no longer be a skiing month by the end of the century.

- In December (Fig. 2.4.6), RCP4.5 is associated with reductions in this ratio of about 10 percent by 2040, while RCP8.5 is associated with reductions of 15 – 20 percent by the same time. By 2095, RCP4.5 indicates a reduction of 20 – 25 percent, while RCP8.5 indicates a reduction of 30 – 40 percent. In particular, the RCP8.5 scenario indicates that, by 2095, only about 30 – 35 percent of all precipitation in December will fall in the form of snow, with the rest falling in some other form. This can be compared to the present, when 60 – 70 percent of total December precipitation falls as snow.

1.5. **Natural snowpack.** As with several of the previous parameters, this one is relatively insensitive to RCP between 2020 and 2040, but important differences emerge by the end of the century.

- In January (Fig. 2.5.1), both RCPs indicate a reduction of about 10 mm (0.4 inch) SWE at all locations by 2040. With RCP4.5, this falls to about 80 mm (3.2 inch) SWE at three locations (Cannon, Loon, and Tenney Mountain), and to about 110 mm (4.4 inch) SWE at Waterville Valley. With RCP8.5, Tenney Mountain and Cannon both fall to less than 40 mm (1.6 inch) SWE by 2095, Loon to about 45 mm (1.8 inch) SWE, and Waterville Valley to about 60 mm (2.5 inch) SWE. At all four locations, the total natural snowpack is reduced by a factor of about 2/3 between 2020 and 2095 with RCP8.5.

- In February (Fig. 2.5.2), RCP4.5 is associated with a reduction of about 10 mm (0.4 inch) SWE by 2040, and RCP8.5 is associated with a reduction of between zero (at Waterville Valley) and 20 – 30 mm (0.8 to 1.2 inches) SWE at the other locations by 2040. By 2095, RCP4.5 produces reductions of about 40 mm (1.6 inch) SWE at all locations, while RCP8.5 produces reductions of about 100 mm (4.0 inch) SWE at all locations. By 2095, Tenney Mountain indicates less than 50 mm (2.0 inch) SWE, Cannon slightly more than 50 mm (2.0 inch) SWE, Loon about 75 mm (3.0 inch) SWE, and Waterville Valley about 100 mm (4.0 inch) SWE. At the four locations, February snowpacks are reduced by between half and two thirds with RCP8.5 between 2020 and 2095.

- In March (Fig. 2.5.3), both scenarios are associated with reductions in snowpack by 2040. RCP4.5 shows reductions of 20 – 40 mm (0.8 to 1.6 inch) SWE, and RCP8.5 shows reductions of about 55 mm (2.2 inch) SWE at all locations. By 2095, RCP4.5 shows reductions of about 50 mm (2.0 inch) SWE, while RCP8.5 is associated with reductions of about 150 mm (6.0 inch) SWE. By 2095, March snowpack with RCP8.5 is as low as about 25 mm (1.0 inch) SWE (at Tenney Mountain) and as high as about 75 mm (3.0 inch) SWE (at Waterville Valley). These are significant reductions from 2020 values of between 150 (6.0 inch) and 250 mm (10.0 inch) SWE.

- April (Fig. 2.5.4) is similar to March. Both scenarios show reductions at all locations by 2040. By 2095, RCP4.5 is associated with reductions of 50 – 90 mm (2.0 to 3.6 inches) SWE, with Waterville showing the largest decrease. With RCP8.5, all four locations indicate that natural snowpack will be reduced to near zero, meaning that April will no longer be part of the ski season by the end of the century.

- In November (Fig. 2.5.5), RCP4.5 is associated with reductions of snowpack by about half at three locations (Cannon, Loon, and Waterville Valley), while Tenney Mountain remains at a relatively low value of 2 mm (0.08 inch) SWE until then. By 2095, RCP4.5 shows modest reductions in snowpack at the same three locations, while Tenney Mountain remains steady at only 2 mm SWE. Under RCP8.5, all locations drop to less than 2 mm SWE by 2095, indicating that, like April, November will no longer be part of the ski season in the region.

- December (Fig. 2.5.6) shows small reductions under RCP4.5 by 2040, while remaining relatively constant under RCP8.5. In the former case, snowpack is reduced by 15 – 20 mm (0.6 to 0.8 inches) SWE at all locations, while remaining steady to slightly increasing during the same period under RCP8.5. By 2095, both RCP4.5 and RCP8.5 are associated with reductions of about 20 mm (0.8 inch) SWE at all four locations. RCP4.5 values by 2095 range from 20 mm (0.8 inch) SWE (at Tenney Mountain) to about 35 mm (1.4 inch) SWE (at the other three locations). RCP8.5 values by 2095 are all at or below 20 mm (0.8 inch) SWE at all locations, corresponding to a reduction by about half of the 2020 values.

2. **Warm-season.**

2.1. Number of days with maximum temperature of 90 °F (32.2 °C) or higher.

- May (Fig. 3.1.1) shows increasing incidents with both RCPs, although, in absolute terms, they remain rare. Loon and Tenney Mountain show the largest increases, increasing from about zero to about two by 2095.

- June (Fig. 3.1.2) shows increasing incidents with both RCPs by the end of the century. With RCP4.5, May incidents approximately double by 2095, and with RCP8.5, incidents increase from about one to between four (at Cannon) and 10 (at Tenney Mountain).

- July (Fig. 3.1.3) and August (Fig. 3.1.4) show the strongest trends, being the hottest months of the year. Once again, the strongest warming trends are evident at Loon and Tenney Mountain, with the latter indicating almost 20 days in both July and August with high temperatures in excess of 90 °F.

- Similar trends are evident in September (Fig. 3.1.5), but are much weaker, with Tenney Mountain indicating only about six days with high temperatures above 90 °F (up from about one in 2020). October (Fig. 3.1.6) also indicates increases by the second half of the century, but the ensemble-average number of days meeting the criteria are well below one.

2.2. **Monthly total precipitation (Figs. 3.2.1 – 3.2.6).** In most cases (by month and RCP), there appears to be fluctuation on warm-season monthly precipitation totals, but no obvious systematic trends. Exceptions are in May, with RCP8.5 indicating significant *increases* toward the end of the century, and in August, with RCP8.5 indicating overall *decreases* toward the end of the century.

2.3. Zero-precipitation events, by number of days.

- Three-day events (Fig. 3.3.1) show increases over the course of the 21st Century with both RCPs. By 2040, all four locations show small increases in the frequency of these events with both RCPs. With RCP4.5, these events increase by about a third at all four locations by 2095, occurring as often as 15 times during the warm season. With RCP8.5, these events approximately double in number by 2095, occurring as often as about 22 times during the warm season.

- Five-day events (Fig. 3.3.2) follow a pattern similar to that of three-day events, although are rarer in terms of absolute numbers. With RCP4.5, these increase slightly by 2040, and approximately double from two to four by 2095. With RCP8.5, the 2040 result is about the same, although they triple (from two to six events) in some locations by 2095.

- Seven-day events (Fig. 3.3.3) show a slight decrease at three of four locations by 2040 with RCP4.5, and a slight increase at all four locations with RCP8.5. Absolute numbers are small: Near unity by 2040, and only totaling as high as about two by 2095.

- Nine-day events (Fig. 3.3.4), 11-day events (Fig. 3.3.5), 13-day events (Fig. 3.3.6) and 15-day events (Fig. 3.3.7) all show totals well below unity throughout the 21st Century. Of interest, although probably not statistically significant, is a peak in the 11-day, 13-day, and 15-day events in the decade between 2070 and 2080.

2.4. **Precipitation events by category.** This parameter was examined twice. During the first pass, the primary focus was on events at the lower end of the scale. The analysis was then repeated, with a finer-scale focus on events in the middle of the scale.

- 24-hr events totaling 2 – 4 mm (0.08 to 0.16 inches) (Fig. 3.4.1) show slight declines at some locations and no changes at other locations by 2040 with both RCPs. By 2095, RCP4.5 is not associated with any important changes, while RCP8.5 is associated with slight decreases at all four locations.

- 24-hr events totaling 4 – 6 mm (0.16 to 0.24 inches) (Fig. 3.4.2) show slight increases at two locations by 2040 with RCP4.5, and at one location with RCP8.5, while decreasing slightly at three locations with RCP8.5. By 2095, RCP4.5 is associated with slight increases at two locations, and RCP8.5 is associated with a slight decrease at all locations.

- 24-hr events totaling 6 to 10 mm (0.25 to 0.4 inches) (Fig. 3.4.3) do not show any important trends with either RCP. Neither do those totaling 10 to 15 mm (0.4 to 0.6 inches) (Fig. 3.4.4), or 15 – 25 mm (0.6 to 1.0 inches) (Fig. 3.4.5). Events of 25 – 50 mm (1.0 to 2.0 inches) (Fig. 3.4.6) show slight upward trends toward the end of the 21st Century with RCP8.5, as do events totaling 50 – 75 mm (2.0 to 3.0 inches) (Fig. 3.4.7). In the remainder of initial categories, the absolute numbers are probably too small to be of statistical significance.

- The re-analysis (in 10-mm, or 0.4-inch increments) indicates a slight upward trend with RCP8.5 in the 50 – 60 mm (2.0 to 2.4 inches) range by the end of the century, although the absolute numbers are once again probably too small to be statistically significant (Fig. 3.5.4).

Summary and Conclusions. Changes in minimum daily temperature during the *cold-season* (November - April) by 2040 are relatively insensitive to RCP, with all four locations showing increases on the order of 1 °C (2 °F) during the six-month period. The results indicate a likely increase in minimum daily temperatures in January of between 3 and 7 °C (about 5 and 13 °F) by the end of the century, depending on RCP. February's and March's results are similar, increasing by between 2 and 6 °C (4 and 11 °F). April's mean monthly minimum temperatures will likely exceed the freezing point of water by mid-century under RCP8.5. November and December are likely to see increases in minimum daily temperatures of between 2 and 5 °C (4 and 9 °F).

Possible impacts on the ski industry in the area were investigated by using the minimum daily temperatures to examine the viability of artificial snowmaking, which can take place with temperatures at -2 °C (28 °F) and below. The results indicate that this is relatively insensitive in January and February to RCP up to 2040, with no important trends in the number of viable days by then. By the second half of the 21st Century, however RCP8.5 is associated with reductions of up to five in the number of viable days during both months. RCP8.5 is associated with even stronger decreases in March, losing up to eight days when snow can be made, and stronger again in April, which sees reductions in the number of viable days from about 15 in 2020 to as few as five by 2095. November sees reductions in the number of viable days with both RCPs by 2040, and by 2095, reductions by about half (falling to between eight and 10 viable days) with RCP8.5. December remains steady under both RCPs by 2040 (each indicating about 30 viable days), but drops by between four and six days with RCP8.5 by 2095. Recall that these results do not indicate the number of *hours* each day when snowmaking will be viable; only that there will be at least one hour during the day when this is true.

Impacts on the area ski industry were also examined by looking at total monthly snowfall during the 21st Century. It was found that neither RCP is associated with reductions in snowfall in January by 2040, but RCP8.5 is associated with reductions in snowfall of 20 mm (0.8 inch) SWE in at least one location by 2095. In February, RCP8.5 is associated with reductions of between 20 and 30 mm (0.8 to 1.2 inches) SWE at all four locations examined by 2095. In March, both RCPs result in small reductions at all four locations by 2040, and by 2095, RCP8.5 is associated with reductions of 30 – 50 mm (1.2 to 2.0 inches) SWE. In April, RCP8.5 is associated with a total loss of natural snowfall by 2095. November also sees strong reductions in snowfall with RCP8.5 by 2095, with one location (Tenney Mountain) receiving none, and the remaining three locations receiving less than 10 mm (0.2 inch) SWE. Even December sees reductions with of about 30 mm (1.2 inch) SWE at all four locations and both RCPs by 2040, and losses of up to 50 mm (2.0 inch) SWE with RCP8.5 by 2095.

The author also examined the ratio of cold-season precipitation falling as snow. The results indicate that by 2095, less than half of January and February precipitation will fall as snow under both RCPs. In March, the results indicate that RCP8.5 will reduce the ratio to about 20 percent by 2095, and in April, RCP8.5 will result in almost all precipitation falling in some form other than snow by 2095. Similar results are found with both RCPs for November. Even December sees reductions in the ratio with both RCPs by 2095: RCP4.5 indicates a reduction by 20 – 25 percent, while RCP8.5 is associated with a reduction by 30 – 40 percent. With RCP8.5, only about a third of December precipitation will fall as snow in 2095, which can be compared to 2020, when 60 – 70 percent falls as snow.

Natural snowpack was examined to determine the impact of changing precipitation types and amounts on snow on the ground. In January, both RCPs indicate reductions of about 10 mm (0.4 inch) SWE by 2040, and losses by as much as 60 mm (2.4 inch) SWE by 2095. February shows a similar trend, with losses reaching 100 mm (4.0 inch) SWE at one location by 2095. March values fall by up to 40 mm (1.6 inch) SWE by 2040, and as much as 250 mm (10 inch) SWE by 2095. And by 2095, April's and November's snowpack values fall to near zero. December remains viable, and indicates reductions of only about 20 mm (0.8 inch) SWE by the end of the century.

Taken together, the results for total snowfall, snowfall ratio, and snowpack indicate that the ski industry will begin to experience stresses by the middle of the 21st Century, and essentially become unviable in April and November at all four locations by 2095. This will reduce our ski season from about five months to about three, and even during the three remaining months, ski resorts will have to cope with degraded snow quality as a result of the increased incidence of non-snow precipitation, losses in the number of days when artificial snow can be made, and diminishing natural snowpack.

The *warm-season* (May - October) results indicate an increase in the number of days with high temperatures reaching 90 °F (32.2 °C) by the second half of the century. Depending on RCP, May sees an increase from essentially none in the present to about two by 2095, and June will experience an increase of up to ten days. July and August will experience up to 20 days exceeding this threshold, and September will increase to as many as six days above the threshold. The results for warm-season total monthly precipitation show small fluctuations throughout, with RCP8.5 producing *increases* during May by the end of the century, and *decreases* during August by 2095. The former probably results from the increased capacity of warmer air to hold more water vapor that can be converted into the precipitation, and the latter probably results from the intensification of the subtropical ridge, which is a stable region of high pressure (often associated with drought) that moves north and intensifies during the summer.

"Droughts" (defined here as contiguous runs of days of a selected length with zero precipitation) were also examined for trends. The results indicate that 3-day droughts will become more common with both RCPs by the end of the century, as will 5-day droughts (although the latter remain relatively rare). Droughts of seven days will also remain rare, but show in a slight increase by 2095. The remaining results (9- through 15 days) are probably not statistically significant.

The last parameter examined was daily precipitation totals, by categories (ranging from 2- 4 mm to more than 100 mm). The results indicate a slight *decrease* in daily totals in the 2 – 4 mm (0.08 to 0.16 inches) and 4 – 6 mm (0.16 to 0.24 inches) ranges with RCP8.5 by 2095, and a slight increase in the 50 – 60 mm (2.0 to 2.4 inches) range with RCP8.5 by the same year. The absolute numbers with the second result are quite small and are probably below statistical significance.

Taken together, the warm-season results indicate that the area will experience a greater number of days when heat stress may have an impact on human health, especially during the months of July and August, that short-term droughts (3- and 5-day duration) will become more common (increasing stresses

on local agriculture), and that precipitation events at the lower end of the spectrum will become somewhat more rare (increasing the relative prevalence of heavier precipitation events).

References.

Burakowski, E., 2020: Personal communication. Dr. Burakowski is a Research Assistant Professor at the Earth Systems Research Center, in the Institute for the Study of Earth, Oceans, and Space, University of New Hampshire.

ClimateNexus, n.d.: RCP8.5: Business-as-usual or a worst-case scenario, accessed July, 2020. [Available on-line at climatenexus.org/climate-change-news/rcp-8-5-business-as-usual-or-a-worst-case-scenario/]

Grogan, D., E. Burakoswki, and A. Contosta, 2020: Snowmelt control on spring hydrology declines as the vernal window lengthens, *Environmental Research Letters*, in review.

Hausfather, Z., 2018: Explainer: How 'Shared Socioeconomic Pathways' explore future climate change, accessed July, 2020. [Available on-line at www.carbonbrief.org/explainer-how-shared-socioeconomic-pathways-explore-future-climate-change]

IPCC Data Distribution Center, 2019: Representative Concentration Pathways (RCPs), accessed July, 2020. [Available on-line at sedac.ciesin.columbia.edu/ddc/ar5_scenario_process/RCPs.html]

Miller, S., 2020: *AirSea* Matlab-based data analysis suite. For more, see http://vortex.plymouth.edu/~stmiller, and follow the link for Matlab:airsea.

NOAA(a), n.d., Climate Model: Temperature Change (RCP 4.5 – 2006 - 2010), accessed July, 2020. [Available on-line at sos.noaa.gov/datasets/climate-model-temperature-change-rcp-45-2006-2100]

NOAA(b), n.d., Climate Model: Temperature Change (RCP 8.5 – 2006 - 2010), accessed July, 2020. [Available on-line at sos.noaa.gov/datasets/climate-model-temperature-change-rcp-85-2006-2100]

Pierce, D., D. Cayan, and B. Thrasher, 2014: Statistical downscaling Using Localized Constructed Analogs (LOCA), *Journal of Hydrometeorology*, **15**, 2558 – 2585.

RCP Database, 2009: RCP Database Version 2.0.5, accessed July, 2020. [Available on-line at www.iiasa.ac.at/web-apps/tnt/RcpDb]

Steffen, W., J. Rockström, K. Richardson, T. Lenton, C. Folke, D. Liverman, C. Summerhayes, A. Barnosky, S. Cornell, M. Crucifix, J. Donges, I. Fetzer, S. Lade, M. Scheffer, R. Winkelmann, and H. Schellnhuber, 2018: Trajectories of the Earth System in the Anthropocene, *Proceedings of the National Academy of Sciences*, **115** (33), 8252–8259, doi:10.1073/pnas.1810141115

Wilson, G., M. Green, and K. Mack, 2018: Historical climate warming in the White Mountains of New Hampshire (USA): Implications for snowmaking water needs at ski areas, *Mountain Research and Development*, **38** (2), 164 - 171, http://dx.doi.org/10.1659/MRD-JOURNAL-D-17-00117